



## Control of *Clostridium difficile* Physiopathology in Response to Cysteine Availability.

Thomas Dubois, Marie Dancer-Thibonnier, Marc Monot, Audrey Hamiot, Laurent Bouillaut, Olga Soutourina, Isabelle Martin-Verstraete, Bruno Dupuy

### ► To cite this version:

Thomas Dubois, Marie Dancer-Thibonnier, Marc Monot, Audrey Hamiot, Laurent Bouillaut, et al.. Control of *Clostridium difficile* Physiopathology in Response to Cysteine Availability.. *Infection and Immunity*, 2016, 84 (8), pp.2389-405. 10.1128/IAI.00121-16 . pasteur-01370880

**HAL Id: pasteur-01370880**

**<https://pasteur.hal.science/pasteur-01370880>**

Submitted on 23 Sep 2016

**HAL** is a multi-disciplinary open access archive for the deposit and dissemination of scientific research documents, whether they are published or not. The documents may come from teaching and research institutions in France or abroad, or from public or private research centers.

L'archive ouverte pluridisciplinaire **HAL**, est destinée au dépôt et à la diffusion de documents scientifiques de niveau recherche, publiés ou non, émanant des établissements d'enseignement et de recherche français ou étrangers, des laboratoires publics ou privés.

Copyright

1 **Control of *Clostridium difficile* physiopathology in response to cysteine availability**

2

3 **Thomas Dubois<sup>1#</sup>, Marie Dancer-Thibonnier<sup>1#</sup>, Marc Monot<sup>1</sup>, Audrey Hamiot<sup>1</sup>,**  
 4 **Laurent Bouillaut<sup>3</sup>, Olga Soutourina<sup>1,2</sup>, Isabelle Martin-Verstraete<sup>1,2,#</sup> and Bruno**  
 5 **Dupuy<sup>1, #,\*</sup>**

6

7 1. Laboratoire Pathogénèse des Bactéries Anaérobies, Institut Pasteur, 25-28, rue du  
 8 Docteur Roux, 75724 Paris Cedex 15, France.

9 2. Université Paris 7-Denis Diderot, 75205 Paris, France

10 3. Department of Molecular Biology and Microbiology, Tufts University School of  
 11 Medicine, Boston, MA, USA

12

13 # These authors contributed equally to this work

14

15

16 Corresponding author: Bruno Dupuy \*

17 E-mail: bdupuy@pasteur

18

19 **Key words:** cysteine metabolism, iron sulfur cluster, oxidative stress, fermentation

20

21 **Running title:** *C. difficile* toxin regulation by cysteine

22

23

## Abstract

The pathogenicity of *Clostridium difficile* is linked to its ability to produce two toxins: TcdA and TcdB. The level of toxin synthesis is influenced by environmental signals, such as PTS sugars, biotin and amino acids, especially cysteine. To understand the molecular mechanisms of cysteine-dependent repression of toxin production, we reconstructed the sulfur metabolism pathways of *C. difficile* strain 630 *in silico* and validated some of them by testing *C. difficile* growth in the presence of various sulfur sources. High levels of sulfide and pyruvate were produced in the presence of 10 mM cysteine, indicating that cysteine is actively catabolized by cysteine desulphydrases. Using a transcriptomic approach, we analyzed cysteine-dependent control of gene expression and showed that cysteine modulates the expression of genes involved in cysteine metabolism, amino-acid biosynthesis, fermentation, energy metabolism, iron acquisition and the stress response. Additionally, sigma factor (SigL) and global regulators (CcpA, CodY, Fur) were tested to elucidate their roles in the cysteine-dependent regulation of toxin production. Among these regulators, only *sigL* inactivation resulted in the de-repression of toxin-gene expression in the presence of cysteine. Interestingly, the *sigL* mutant produced less pyruvate and H<sub>2</sub>S than the wild-type strain. Unlike cysteine, the addition of 10 mM pyruvate to the medium for a short time during the growth of the wild-type and *sigL* mutant strains reduced expression of the toxin gene, indicating that cysteine-dependent repression of toxin production is mainly due to the accumulation of cysteine by-products during growth. Finally, we showed that the effect of pyruvate on toxin-gene expression is mediated at least in part by the two-component system CD2602-CD2601.

## Introduction

*Clostridium difficile* is a Gram-positive spore-forming obligate anaerobe and the major cause of nosocomial diarrhea associated with antibiotic therapy. The symptoms of *C. difficile* infection (CDI) vary from mild diarrhea to life-threatening pseudomembranous colitis, a severe form of CDI (1). Virulent *C. difficile* strains produce two large toxins, an enterotoxin (TcdA) and a cytotoxin (TcdB). The *tcdA* and *tcdB* genes are clustered within a single chromosomal region called the pathogenicity locus (PaLoc) with three accessory genes, *tcdR*, *tcdE* and *tcdC*. The expression of the toxin genes is controlled through the coordinated action of the alternative sigma factor TcdR and its antagonist factor TcdC (2-4). The *tcdE* gene encodes a holin-like protein that is required for toxin release (5).

The spectrum of diseases caused by *C. difficile* depends on host factors and, for the severe forms, on the level of toxins produced, suggesting that the regulation of toxin synthesis is a critical determinant of *C. difficile* pathogenicity (6). Toxin production starts when *C. difficile* cultures enter the stationary growth phase (7) and is modulated in response to various environmental signals. Exposure to subinhibitory concentrations of antibiotics, a temperature of 37°C, biotin limitation or the presence of butyric acid stimulates toxin production (8, 9). By contrast, the presence of rapidly metabolized carbon sources, such as glucose and butanol, or amino acids, such as cysteine and proline, inhibit toxin synthesis (7, 10-12). Some of the molecular mechanisms regulating *C. difficile* toxin synthesis in response to environmental signals have been elucidated (13-16). It has been shown that CodY, the global regulator involved in the adaptive response to nutrient limitation, represses toxin-gene expression by binding to the *tcdR* promoter region (14, 17) and that glucose-dependent repression of toxin production is mediated by CcpA, the global regulator of carbon catabolite repression (CCR) (13). This repression is the result of the direct binding of CcpA to a *cis*-acting catabolite response element (*cre* site) that is present in the regulatory regions of the *tcdA*, *tcdB*, *tcdR* and *tcdC* genes, with the strongest affinity observed for the *tcdR* promoter (18). Toxin-gene expression also depends on transcriptional factors, such as SigH and Spo0A, which control the transition to the post-exponential growth phase and the initiation of sporulation (15, 16).

Changes in colonic flora after antibiotic treatment lead to the modification of metabolic pools, which affects the spore germination and cell growth of *C. difficile* (19).

Specifically, the levels of several PTS sugars, such as mannitol and sorbitol, and amino acids, such as proline, cysteine and cystine, the cysteine dimer, increase during gut dysbiosis. These compounds are metabolized by *C. difficile* and may serve as metabolic signals that are detected by regulators to coordinate adaptation, growth and virulence-factor production during gut colonization.

Among the amino acids that down-regulate toxin production in *C. difficile* strains, cysteine is the most potent (11, 12). Links between bacterial virulence and cysteine metabolism have been described in several pathogenic bacteria. In *Clostridium perfringens* and *Bordetella pertussis*, toxin synthesis is regulated in response to cysteine availability (20, 21). Additionally, genes involved in sulfur metabolism are induced when *Mycobacterium tuberculosis*, *Yersinia ruckeri*, *Staphylococcus aureus* and *Nesseiria meningitidis* interact with human cells (22-24). In addition, loss-of-function mutations in genes involved in cysteine biosynthesis or degradation affect the virulence for some of these pathogens (23-26). Finally, the master regulator of cysteine metabolism in *S. aureus*, CymR, plays an important role in both the stress response and the control of bacterial virulence (27).

The sulfur-containing amino acid cysteine is central to bacterial physiology. This amino acid is a precursor of methionine and of several co-enzymes (biotin, thiamine, coenzyme A and coenzyme M). Cysteine is also the sulfur donor for the biogenesis of the iron-sulfur (Fe-S) clusters that are found in the catalytic site of several enzymes and assists in protein folding and assembly by forming disulfide bonds. Moreover, cysteine-containing proteins (thioredoxin, glutaredoxin) and molecules (glutathione, bacillithiol, mycothiol) are important in protecting cells against oxidative stress (28, 29). Two major cysteine biosynthetic pathways are present in microorganisms: i) the thiolation pathway, which directly incorporates sulfide or thiosulfate into *O*-acetyl-L-serine (OAS), and ii) the reverse transsulfuration pathway, which converts homocysteine into cysteine via a cystathionine intermediate (Fig. 1) (30, 31). Homocysteine is synthesized from methionine using the S-adenosyl-methionine (SAM) recycling pathway, while sulfide arises mostly from the reduction of sulfate.

Due to the reactivity of its thiol group, the intracellular concentration of cysteine must be tightly controlled. The pathways responsible for depleting free cysteine include those that incorporate cysteine into molecules (proteins, methionine, Fe-S clusters, vitamins) and those that degrade or export it (30). Cysteine can also be catabolized by cysteine desulphydrases or cysteine desulfidase, producing pyruvate and hydrogen sulfide

113 (H<sub>2</sub>S) (Fig. 1) (24, 32). Finally, a large variety of molecular mechanisms participate in fine-  
114 tuning cysteine metabolism in response to environmental changes. These systems include  
115 regulation by the premature termination of transcription at T-box systems in response to  
116 the level of charge of tRNA<sub>Cys</sub> (33) or by several transcriptional regulators, including  
117 activators of the LysR family (30) and CymR, a repressor of the Rrf2-family (34, 35).

118  
119 To understand the molecular mechanisms involved in the cysteine response, we  
120 performed a reconstruction of *C. difficile* sulfur metabolism and analyzed the global effect  
121 of cysteine on gene expression. Then, we showed that cysteine-dependent repression of  
122 toxin production requires SigL. Moreover, we observed that the production of pyruvate  
123 and H<sub>2</sub>S decreased in the *sigL* mutant compared to the wild-type strain. Interestingly,  
124 addition of pyruvate to the growth medium of the wild-type and the *sigL* mutant strains  
125 repressed toxin-gene transcription, suggesting that the effect of cysteine on toxin  
126 production is due, at least in part, to the accumulation of cysteine by-products resulting  
127 from cysteine degradation. Finally, we showed that the regulation of toxins by exogenous  
128 pyruvate is mediated by a two-component system (TCS) through a still uncharacterized  
129 mechanism.

## 130 131 **Materials and Methods**

### 132 133 **Bacterial strains and culture conditions**

134 The *C. difficile* strains used in this study are described in Table 1. *Escherichia coli* strain  
135 NEB-10 beta (BioLabs) and *E. coli* strain HB101 (RP4) were used, respectively, for cloning  
136 and as a donor strain for *C. difficile* conjugation experiments. *C. difficile* strains were  
137 grown anaerobically (5% H<sub>2</sub>, 5% CO<sub>2</sub>, 90% N<sub>2</sub>) in PY (Bacto peptone (20g/l); Yeast extract  
138 (10g/l); CaCl<sub>2</sub> 0.4% (2ml/l); Resazurine 0.025% (4m/l); Hemin 0.05% (10ml/l); Vitamin  
139 K 0.05% (1m/l) and 40ml/l of salts solution (K<sub>2</sub>HPO<sub>4</sub> (1g/l), KH<sub>2</sub>PO<sub>4</sub> (1g/l), NaHCO<sub>2</sub>  
140 (10g/l), NaCl (2g/l), MgSO<sub>4</sub>·7H<sub>2</sub>O (0.2g/l)), PYC (PY with 10 mM cysteine) or PYHC (PY  
141 with 10 mM homocysteine) media (12). After 9 h of cell growth, 15 mM of acetate or 10  
142 mM of pyruvate, Na<sub>2</sub>S or formate were added to the PY medium. When necessary,  
143 cefoxitin (25 µg/ml), thiamphenicol (15 µg/ml) or erythromycin (2.5 µg/ml) were added  
144 to *C. difficile* cultures. *E. coli* strains were grown in Luria-Bertani (LB) broth. When  
145 indicated, ampicillin (100 µg/ml) or chloramphenicol (15 µg/ml) was added to the

146 culture medium. Additionally, 200 ng/ml of anhydrotetracycline (Atc) was used to induce  
147 the  $P_{tet}$  promoter of the pRPF185 vector derivatives in *C. difficile* (36). The sulfur-free  
148 minimal medium was as previously described (20), with the addition of 0.3 g/L of proline.  
149 The concentrations of the sulfur sources added are indicated in Table 2.

#### 150 **Dot-blot analysis**

151 Crude extracts were obtained using the FastPrep® (MP Biomedicals) cell-lysis system  
152 (speed 6, time 40, performed twice), followed by centrifugation (10 min at 4°C) to remove  
153 cell debris. For dot-blot experiments, 20 ng (VPI10463) or 200 ng [630 $\Delta$ erm, M7404 and  
154 M7404 (*tcdC*<sup>+</sup>)] of proteins from the crude extracts were directly spotted onto a  
155 nitrocellulose membrane (Hybond-C extra, Amersham Biosciences). The membranes  
156 were blocked with 5% w/v non-fat dried milk in Tris-buffered saline (TBS) supplemented  
157 with 0.2% (v/v) Tween-20 (TBST) for 1 h at room temperature (RT). The membranes  
158 were then incubated for 90 min at 37°C with the TcdA antibody (PCG-4, Santa Cruz,  
159 Biotechnology) and visualized as described by Antunes et al. (13).

#### 160 **Cell cultures and cytotoxicity assays**

161 Vero cells were cultured in Dulbecco's modified Eagle's medium (DMEM; Gibco)  
162 supplemented with 5% (v/v) fetal calf serum and a 1% ready-to-use solution (v/v) of  
163 penicillin [10 000 U ml<sup>-1</sup>] and streptomycin [10 mg ml<sup>-1</sup>] (Sigma) at 37°C in 5% CO<sub>2</sub>  
164 atmosphere. For cytotoxicity assays, cells were grown until confluence in 96-well plates  
165 and incubated with two-fold serially diluted *C. difficile* crude extracts in DMEM. After 24 h  
166 at 37°C, the cytopathic effect was evaluated using an optical microscope. Positive toxin  
167 reactions were indicated by the characteristic rounding of Vero cells. The titer of each  
168 sample corresponds to the well containing 50 % round Vero cells.

#### 169 **Detection and quantification of hydrogen-sulfide and pyruvate production**

170 H<sub>2</sub>S production was detected using lead-acetate paper (Macherey-Nagel), which turns  
171 black in the presence of this compound. Cells were grown in PY, PYC or PYHC to an  
172 OD<sub>600nm</sub> of 0.7. Then, the lead-acetate paper was placed at the bottom of the flask for 1  
173 min to 1 h at 37°C, depending on the experiment. H<sub>2</sub>S production was further quantified  
174 as previously described (31, 37). Briefly, 5 ml of the 630 $\Delta$ erm strain culture was  
175 introduced into a flask with an alkaline agar layer enriched with zinc acetate and was  
176 incubated for 1 h at 37°C. The OD<sub>670nm</sub> was measured against an H<sub>2</sub>O blank. The amount of

177 H<sub>2</sub>S was calculated using a standard curve of Na<sub>2</sub>S. For pyruvate quantification, cells were  
178 grown in PY or PYC for 10 h at 37°C, and pyruvate was quantified in the supernatant using  
179 a Pyruvate Assay Kit (Sigma). The final pyruvate concentration was standardized using  
180 the OD<sub>600nm</sub> of the bacterial cultures.

### 181 **Estimation of the intracellular amino-acid content**

182 The intracellular concentrations of amino acids were estimated using high-pressure liquid  
183 chromatography (HPLC) (31, 38). Briefly, cells were suspended in a sulfosalicylic acid  
184 buffer (3% final concentration) and disrupted using a Fastprep apparatus (MP  
185 Biomedicals). After centrifugation, supernatant samples were analyzed by cation-  
186 exchange chromatography, followed by ninhydrin postcolumn derivatization as  
187 previously described (31).

### 188 **Zymogram**

189 Zymograms were performed to detect the cysteine desulfhydrase and homocysteine g-  
190 lyase activities. Native protein crude extracts (40 and 100 µg, respectively) were run on a  
191 non-denaturing protein gel (12% polyacrylamide in Tris-Glycine buffer). After  
192 electrophoresis, the gel was incubated at 37°C for one to four hours in a Tris solution (50  
193 mM Tris-HCl (pH 7.4), 10 mM MgCl<sub>2</sub>, 0.5 mM Pb(NO<sub>3</sub>)<sub>2</sub> and 5 mM DTT) with 0.4 mM  
194 pyridoxal-5-phosphate (PLP) containing either 10 mM L-cysteine or 10 mM homocysteine  
195 as previously described (32). H<sub>2</sub>S formed by the cysteine desulfhydrase or homocysteine  
196 γ-lyase activity precipitates as insoluble PbS.

### 197 **Construction of *C. difficile* mutants**

198 The ClosTron gene-knockout system (39) was used to inactivate genes encoding Fur  
199 (*CD1287*), SigL (*CD3176*), CysK (*CD1594*) and a TCS-sensor histidine kinase (*CD2602*), as  
200 well as several regulators of unknown function (*CD2065*, *CD0278* and *CD2023*; Table 1).  
201 As described in Fig. S1, primers were designed to retarget the group-II intron of  
202 pMTL007 to these genes (Table S1) and were used to generate a 353-bp DNA fragment  
203 by overlap PCR according to the manufacturer's instructions. These PCR products were  
204 cloned into the *Hind*III and *Bsr*GI restriction sites of the pMTL007 and were verified by  
205 DNA sequencing using the pMTL007-F and pMTL007-R primers (Table S1). The derived  
206 pMTL007 plasmids were transformed into *E. coli* strain HB101 (RP4) and transferred by  
207 conjugation into the *C. difficile* strain 630Δ*erm*. *C. difficile* transconjugants were selected

208 by sub-culture on BHI agar containing thiamphenicol (15 µg/ml), and the integration of  
209 the group-II intron RNA into genes was induced and selected by plating onto BHI agar  
210 containing erythromycin (2.5 µg/ml). The chromosomal DNA of the transconjugants was  
211 extracted using the InstaGene Kit (BioRad), and PCR using the primers ErmRAM-F and  
212 ErmRAM-R (Table S1) was used to confirm the erythromycin-resistant phenotype due to  
213 the splicing of the group-I intron from the group-II intron following integration (Fig.  
214 S1A). The insertion of the group-II intron into target genes was verified by Southern blot  
215 (Fig. S1C) and by PCRs (Fig. S1B) with primers flanking the 5' ends of genes (Table S1)  
216 and EBSu primer. To knock down *maly* (*CD3029*) expression, a DNA fragment  
217 comprising the 5' untranslated region (UTR) and the beginning of the *CD3029* open  
218 reading frame (-38 to +154 from the ATG start codon) was amplified by PCR and cloned  
219 between the *XhoI* and *BamHI* sites of the pRPF185 vector (36) to generate pDIA6456  
220 expressing the 5' end of *maly* in the antisense orientation under the control of the ATc-  
221 inducible *P<sub>tet</sub>* promoter. This plasmid was transferred by conjugation into *C. difficile*  
222 strain 630Δ*erm*. To complement the *sigL* mutant, the *sigL* gene and its promoter (-193 to  
223 +1380 from the ATG start codon) were amplified by PCR using the appropriate primers  
224 (Table S1). The PCR fragment was cloned into the *XhoI* and *BamHI* sites of pMTL84121  
225 (40) to generate plasmid pDIA6309. This plasmid was transferred by conjugation into  
226 the *C. difficile sigL* mutant (CDIP217), yielding strain CDIP342.

227 All experiments conducted with the mutants were standardized versus the wild type for  
228 the culture growth (OD<sub>600</sub>) and the protein concentration of the samples or by using a  
229 reference gene for the qRT-PCR assays.

### 230 RNA isolation and quantitative real-time PCR

231 *C. difficile* strains were grown in PY or PYC for 10 h. Total RNA extraction was performed  
232 using the FastRNA Pro Blue kit and a Fastprep apparatus according to the manufacturer's  
233 instructions (MP Biomedicals) as previously described (13). To synthesize cDNA, 1 µg of  
234 total RNA was heated at 70°C for 10 min in the presence of 1 µg of hexamer  
235 oligonucleotide primers (pdN<sub>6</sub>, Roche). RNAs were then reverse transcribed for 2 h at  
236 37°C using AMV Reverse transcriptase (RT) (Promega), 20 mM dNTPs and 40 U of RNasin  
237 (Promega). Reverse transcriptase was inactivated by heating at 85°C for 5 min. Real-time  
238 quantitative RT-PCR was performed in a 20-ml reaction volume containing 20 ng of  
239 cDNAs, FastStart SYBR Green Master mix (ROX, Roche) and 200 nM of gene-specific

240 primers (Table S1). Amplification and detection were performed as previously described  
241 (13). The quantity of each cDNA was normalized to the quantity of the cDNA of the DNA  
242 *polIII* gene (CD1305). The relative change in gene expression was recorded as the ratio to  
243 normalized target concentrations ( $\Delta\Delta Ct$ ) (41). Shapiro-Wilk test was performed to test  
244 the normality of the replicates for each condition (Table S3). When population of the two  
245 conditions was normally distributed a t-test was used, otherwise we used a Mann-  
246 Whitney test as indicated in the legend of figures. A p-value  $\leq 0.05$  was considered  
247 significant.

#### 248 **Microarray design for the *C. difficile* genome, DNA-array hybridization and data** 249 **analysis.**

250 The microarray of the *C. difficile* strain 630 genome was designed as previously described  
251 (15) (GEO database accession number [GPL10556](https://www.ncbi.nlm.nih.gov/geo/query/acc.cgi?acc=GPL10556)). The transcriptome was performed  
252 with four different RNA preparations and a dye-swap method. First, 10  $\mu$ g of total RNA  
253 was reverse transcribed in cDNA using the SuperScript Indirect cDNA labeling system kit  
254 (Invitrogen) and Cy3 or Cy5 fluorescent dye (GE Healthcare) according to the  
255 manufacturer's recommendations. Labeled DNA hybridization to microarrays and array  
256 scanning were performed as previously described (15). The complete experimental data  
257 set was deposited in the GEO database with accession number GSE22423. All slides were  
258 analyzed using the R and limma software (Linear Model for Microarray Data) from the  
259 Bioconductor project ([www.bioconductor.org](http://www.bioconductor.org)). For each slide, we corrected for  
260 background with the 'normexp' method (42), which resulted in strictly positive values  
261 and reduced variability in the log ratios for genes with low hybridization signal levels.  
262 Then, we normalized each slide by the 'loess' method (43). To test for differential  
263 expression, we used Bayesian adjusted t-statistics and performed the multiple-testing  
264 correction of Benjamini & Hochberg based on the false discovery rate (FDR) (44). A gene  
265 was considered to be differentially expressed when the p-value was  $< 0.05$ .

#### 266 **Raw sequences analysis**

267 The presence of the TCS locus (CD2602-26021) was inferred from raw sequences of 2424  
268 published strains (Sequence Read Archive (SRA) accession numbers: PRJEB2039,  
269 PRJEB4556, PRJEB3010, PRJEB190-216, PRJEB6600-2, PRJEB6575). For that purpose, we  
270 mapped the sequencing reads of each strain onto the nucleotide sequence of the TCS locus

271 using Bowtie (1). A strain was considered to contain the TCS locus when the coverage was  
272 above 80%.

273

## 274 **Results & discussion**

275

### 276 **Cysteine-dependent repression of PaLoc genes**

277 It has been shown that toxin synthesis is repressed by cysteine in the high-toxin-level-  
278 producing strain VPI10463 (12). To determine whether the effect of cysteine on toxin  
279 synthesis is strain-dependent, we measured the effect of cysteine on toxin production in  
280 several *C. difficile* backgrounds (Table 1), such as strains 630 $\Delta$ erm and M7404 (a  
281 NAP1/027 epidemic strain), as well as a M7404-derivative strain carrying a wild-type  
282 copy of the *tcdC* gene on the pDLL17 plasmid (2); VPI10463 was used as a control. All of  
283 the strains grew similarly in PY with or without cysteine. Cell crude extracts were  
284 obtained from these four strains after 10 h of growth in PY or PYC, and toxin production  
285 was assayed by Vero cell cytotoxicity assays, which predominantly assess TcdB, and  
286 protein dot-blot analysis using a specific antibody raised against TcdA. Cytotoxic activity  
287 was lower in cells grown in the presence of cysteine (Fig. 2A) compared to cells grown  
288 without cysteine, with 25- to 125-fold decreased cytotoxicity for strains 630 $\Delta$ erm, M7404  
289 and M7404 + pDLL17-*tcdC* and 16000-fold decreased cytotoxicity for strain VPI10463.  
290 Moreover, TcdA accumulation was strongly reduced in the presence of cysteine in all of  
291 the strains tested (Fig. 2B). These results suggest that cysteine-dependent repression of  
292 toxin production is conserved among the *C. difficile* strains. Cysteine repressed toxin  
293 synthesis in both the epidemic 027 strain M7404, which does not express functional TcdC,  
294 and in its derivative strain that contains a wild-type *tcdC* gene (2). Thus, the effect of  
295 cysteine on toxin production is not mediated by TcdC.

296 To determine whether the effect of cysteine on toxin production occurred at the  
297 transcriptional level, we performed qRT-PCR experiments for the *tcdA*, *tcdB* and *tcdR*  
298 genes using strain 630 $\Delta$ erm (Fig. 2C). After 10 h of growth, transcript level of *tcdA* and  
299 *tcdB* decreased 18- and 17-fold, respectively, in the presence of cysteine. We also  
300 observed that the expression of the *tcdR* gene encoding the alternative sigma factor  
301 required for toxin-gene transcription decreased 40-fold when cysteine was added (Fig.  
302 2C). These data are in agreement with the results obtained by Karlsson et al. (11),

303 suggesting that toxin-gene transcription is repressed by cysteine through negative  
304 regulation of *tcdR*.

### 305 **Reconstruction of sulfur metabolism in *C. difficile***

306 An understanding of sulfur metabolism was a prerequisite to elucidating how cysteine  
307 negatively regulates toxin production. To reconstitute the sulfur-metabolism pathways,  
308 we first searched for all of the gene homologs to the genes involved in sulfur-assimilation  
309 pathways in other firmicutes (30) in the complete genome sequence of the reference *C.*  
310 *difficile* strain 630 (45) (Fig. 3). All genes identified are conserved in the VPI10463 and  
311 NAP1/027 epidemic strains (Table S4). Then, to support the metabolic reconstruction  
312 and to obtain new insights about the physiology of *C. difficile*, we tested the ability of  
313 strain 630 $\Delta$ *erm* to grow in minimal media with different sulfur sources (Table 2).

314 Strain 630 $\Delta$ *erm* cannot grow when sulfate is the only sulfur source (Table 2). This finding  
315 is consistent with the absence of genes involved in the first steps of the sulfate-  
316 assimilation pathway leading to sulfite (Fig. 1). By contrast, strain 630 $\Delta$ *erm* was able to  
317 grow in the presence of sulfide or thiosulfate (Table 2), indicating that *C. difficile* can  
318 synthesize cysteine from these compounds, probably through the CysE/CysK thiolation  
319 pathway (Fig. 3). Cysteine can also be produced from glutathione, a sulfur source utilized  
320 by strain 630 $\Delta$ *erm* (Table 2). PepT and PepA are probably involved in the degradation of  
321 glutathione to form cysteine (Fig. 3). However, the pathway of glutathione synthesis from  
322 cysteine that is found in *C. perfringens* (20) is absent in *C. difficile*. Strain 630 $\Delta$ *erm* can also  
323 grow with cysteine as the sole sulfur source, indicating that methionine is efficiently  
324 produced from this compound. As shown in Fig. 3, methionine is synthesized from  
325 homocysteine, likely through the cobalamine-dependent methionine synthase MetH. The  
326 two main pathways of homocysteine production in bacteria are transsulfuration and  
327 thiolation (Fig. 1) (30). Both pathways involve PLP-dependent enzymes: transsulfuration  
328 requires a cystathionine  $\gamma$ -synthase and a cystathionine  $\beta$ -lyase, while thiolation requires  
329 an *O*-acetyl-homoserine (OAH)-thiol-lyase (Fig. 1). In the genome of strain 630, three PLP-  
330 dependent enzymes were identified by their similarities: MetY, MalY and MdeA (46). MetY  
331 contains an amino-acid insertion specific to OAH-thiol-lyases, MalY is a cystathionine  $\beta$ -  
332 lyase of the PatB/MalY family (32), and MdeA is a probable methionine  $\gamma$ -lyase. However,  
333 no cystathionine  $\gamma$ -synthase is present in *C. difficile*, suggesting that a functional

transsulfuration pathway is absent and that *C. difficile* synthesizes both methionine and cysteine by thiolation pathways.

### Homocysteine and Cysteine degradation

Strain 630 $\Delta$ *erm* can grow in the presence of homocysteine and, to a lesser extent, in the presence of cystathionine, but cannot use methionine as the sole sulfur source (Table 2). The ability to use homocysteine is surprising because the reverse transsulfuration pathway, which involves a cystathionine  $\beta$ -synthase and a cystathionine  $\gamma$ -lyase (Fig. 1), is absent in *C. difficile* (31, 47). Growth in the presence of homocysteine could be explained by the existence of a homocysteine  $\gamma$ -lyase, allowing the production of H<sub>2</sub>S from homocysteine and its possible conversion into cysteine (Fig. 3). Using lead-acetate paper, we detected the production of H<sub>2</sub>S during the growth of strain 630 $\Delta$ *erm* in PY plus homocysteine (PYHC), but not in PY alone (Fig. 4A). When we performed a zymogram using homocysteine as a substrate, we detected a single band in crude extracts of strain 630 $\Delta$ *erm* grown in PY, PYC and PYHC (Fig. 4B), suggesting that homocysteine  $\gamma$ -lyase activity is induced in all of the growth conditions used. Among the PLP-dependent enzymes encoded by the *C. difficile* genome, MdeA shares significant similarities with the methionine  $\gamma$ -lyases of *Citrobacter freundii* (48) and of *Brevibacterium linens*. Interestingly, the methionine  $\gamma$ -lyase of *B. linens* also has homocysteine  $\gamma$ -lyase activity (49), making MdeA a probable candidate for the production of H<sub>2</sub>S from homocysteine and the degradation of methionine to form methanethiol in *C. difficile* (Fig. 3), as previously proposed (50).

In bacteria, cysteine is usually catabolized by cysteine desulhydrases (32), producing H<sub>2</sub>S, pyruvate and ammonia (Fig. 1). We detected high production of H<sub>2</sub>S during the growth of strain 630 $\Delta$ *erm* in PYC (Fig. 4A). Indeed, the quantification of H<sub>2</sub>S showed a 20- to 30-fold increase of H<sub>2</sub>S production when cysteine was added to the medium (Fig. 4C). This result clearly indicated that cysteine is efficiently degraded in *C. difficile*. To detect the cysteine desulhydrase activities, we performed a zymogram using L-cysteine as substrate. We detected two bands ( $\alpha$  and  $\gamma$ ) in the crude extract of strain 630 $\Delta$ *erm* grown in PY (Fig. 4D, lane 1). Interestingly, when strain 630 $\Delta$ *erm* was grown in PYC, we detected an additional band ( $\beta$ ), indicating that synthesis of this desulhydrase enzyme was induced by cysteine (Fig. 4D, lane 2). In *B. subtilis*, PatB/MaLY- and CysK-type enzymes have cysteine desulhydrase activities (32). To determine whether CysK of *C. difficile* is a

cysteine desulfhydrase, we inactivated the *cysK* gene in strain 630 $\Delta$ *erm* using the ClosTron system (Fig. S1). The zymogram profile obtained with the *cysK* mutant strain grown in PYC is similar to that obtained with the 630 $\Delta$ *erm* strain (Fig. 4D, lane 3). This finding suggests that CysK is not a major cysteine desulfhydrase in *C. difficile* under the conditions tested, although we cannot exclude a role for CysK in cysteine degradation. We failed to inactivate the gene encoding the PatB/MalY enzyme, probably because of its essentiality for *C. difficile* (51). Thus, to evaluate whether PatB/MalY is a cysteine desulfhydrase, we constructed a PatB/MalY-depleted strain using an antisense strategy (36, 52). Compared to the strain carrying the control plasmid (Fig. 4D lane 5), the PatB/MalY-depleted strain (Fig. 4D lane 6) displayed a decreased intensity of the  $\alpha$  band, suggesting that MalY has cysteine desulfhydrase activity. However, the enzymes with cysteine desulfhydrase activity corresponding to  $\gamma$  and  $\beta$  bands on the zymogram (Fig. 4D) remain to be identified.

Finally, we demonstrated that both homocysteine and cysteine are actively catabolized by *C. difficile*. Interestingly, it has recently been shown that when *C. difficile* grows in minimal media with casminoacids, cysteine is consumed immediately and sulfide is produced (53). This finding is in complete agreement with our results. Thus, we propose that sulfide is a central compound of sulfur metabolism in *C. difficile*, as it is the direct precursor of both methionine and cysteine, as well as the major degradation product of the sulfur-containing amino acids homocysteine and cysteine (Fig. 3).

#### Global analysis of genes expression in response to cysteine

To determine the global impact of cysteine on gene expression and to elucidate the mechanism of cysteine-dependent repression of toxin production, we performed a comparative transcriptional analysis of strain 630 $\Delta$ *erm* grown in PY or PYC at the onset of stationary phase (10 h). In the presence of 10 mM cysteine, 6 % of the genome (201 genes) was differentially expressed with a fold change  $\geq 2$  (Table S2). Among these genes, 120 and 81 were up- and down-regulated, respectively. The major expression changes were seen in genes encoding cell-surface-associated proteins and proteins involved in sulfur, amino-acid, carbon and energy metabolism as well as in iron uptake (Table S2). The transcriptomic analysis confirmed that toxin-gene expression decreased in the presence of cysteine. In addition, exposure of *C. difficile* to high cysteine concentrations strongly induced the expression of genes encoding heat-shock proteins belonging to both

398 Class I (HrcA-dependent), such as the *groESL* and *hrcA* operons, and Class III (CtsR-  
399 dependent), such as the *ctsR* and the *clpB* operons. We validated the transcriptomic  
400 analysis by performing qRT-PCR with a selection of 12 representative genes. The results  
401 confirmed the microarray data (Table S2).

#### 402 **Regulation of genes involved in sulfur metabolism and in thiol protection by** 403 **cysteine**

404 As expected, the expression of genes related to sulfur metabolism, including transporters  
405 of amino acids, was controlled by cysteine. The *metQ<sub>1</sub>* gene encoding the methionine-  
406 binding protein of an ABC transporter (54, 55) (Fig. 3) was less strongly expressed in PYC.  
407 This gene is probably regulated by a S-box riboswitch in the promoter region of the  
408 *metN<sub>1</sub>Q<sub>1</sub>* operon, like most of the genes required for methionine uptake (Fig. 3) (55, 56).  
409 The ABC transporter system composed of CD2177, CD2176, CD2175, CD2174 and  
410 CD2172 is likely involved in the uptake of cystine and/or cysteine in *C. difficile* (Fig. 3).  
411 CD2177 and CD2174 share similarities with the cystine-binding proteins of *E. coli* and *B.*  
412 *subtilis* (57), while CD2176 and CD2175 are similar to the L-cystine permeases of *E. coli*  
413 and *B. subtilis*. The expression of ~~all~~ of the genes encoding this ABC transporter decreased  
414 2.5- to 4-fold in PYC, as is usually observed for cysteine/cystine transporters. By contrast,  
415 the expression of the *ssuA<sub>2</sub>* and *ssuC<sub>2</sub>* genes, which encode proteins sharing similarities  
416 with sulfonate ABC transporters, increased in the presence of cysteine (Fig. 3).

417 The expression of CysK encoding the OAS-thiol-lyase and CysE, the serine acetyl-  
418 transferase was induced 40- to 50-fold in the presence of cysteine (Fig. 3 and Table S2).  
419 The up-regulation of *cysKE* expression in PYC is surprising because CysK and CysE, which  
420 are required for cysteine biosynthesis, are usually induced during cysteine limitation, as  
421 previously observed in *C. perfringens*, *B. subtilis*, *E. coli* and *Salmonella* (20, 30, 34).  
422 However, in the presence of high cysteine concentrations, CysK contributes to cysteine  
423 degradation rather than cysteine synthesis (58). Under these conditions, CysE activity is  
424 inhibited by feedback, as established in several bacteria and plants (38, 59). Nonetheless,  
425 the role of CysK in cysteine metabolism remains to be clarified.

426 Finally, we observed that genes involved in thiol protection were induced in the presence  
427 of cysteine (Table S2). They encode two thioredoxins (*CD1690* and *CD2355*), a thioredoxin  
428 reductase (*CD1691*) and a thiol peroxidase (*CD1822*). The induction of genes involved in  
429 thiol protection and in the stress response suggests that cysteine or its derivative

430 products (e.g., H<sub>2</sub>S) stress *C. difficile*. However, the addition of 10 mM cysteine to the PY  
431 medium did not affect *C. difficile* growth and cell viability (data not shown) while this  
432 amino acid is toxic in other bacteria, such as *E. coli* and *B. subtilis* ((60); I. Martin-  
433 Verstraete, unpublished results). The expression of the stress-responsive genes in  
434 relation to the absence of cysteine toxicity in *C. difficile* may be the result of an adaptation  
435 to an anaerobic lifestyle.

#### 436 **Induction of *fur* and Fur-regulated genes in the presence of cysteine**

437 The ferric uptake regulator (Fur) protein is an iron-response repressor that controls the  
438 expression of genes involved in iron transport in bacteria (61, 62). The CD1287 protein  
439 shares 48 % identity with the Fur protein of *B. subtilis*. To demonstrate that CD1287  
440 corresponds to Fur, we constructed a *CD1287* mutant strain using the ClosTron system  
441 (Fig. S1). Then, we tested the effect of *CD1287* disruption on the level of transcription of  
442 the *feoB1* and *fhuD* genes by qRT-PCR. In *B. subtilis*, FeoB1 and FhuD participate in ferrous  
443 iron and ferrichrome uptake, respectively (61, 63). We showed that the addition of 200  
444 mM of dipyrldyl, a ferrous iron chelator, to the growth medium increased the transcript  
445 level of the *CD1287*, *fhuD* and *feoB1* genes and that transcription of *feoB1* and *fhuD*  
446 increased 3500- and 45-fold, respectively, in the *CD1287* mutant compared to the wild-  
447 type strain (data not shown). These results strongly indicate that CD1287 is the Fur  
448 repressor in *C. difficile*, as recently demonstrated (64).

449 From our global transcriptomic analysis, we found that the presence of cysteine in the  
450 medium induced the Fur-regulon, including *fur* and genes encoding transporters of  
451 ferrous iron and ferrichrome (Table 3). Using the Fur-binding site of *B. subtilis* (61), we  
452 detected a potential Fur box upstream of approximately 20 genes that are differentially  
453 expressed in PYC, including *fur*, *feoB1*, *cysK* and *fhuD*, as well as genes encoding proteins  
454 of unknown function, such as *CD2992*, *CD1485*, *CD2499* and *CD2881* (Table 3). The  
455 consensus Fur box for *C. difficile* (Fig. 5A), deduced from the putative Fur-binding motifs  
456 present in the regulatory region of these genes, is highly similar to that defined by Ho et  
457 al. (64). We then tested the effect of cysteine on the transcription of some of these Fur  
458 targets by qRT-PCR in both 630 $\Delta$ *erm* and a *fur* mutant strain. In the presence of cysteine,  
459 the transcript level of *fur*, *feoB1*, *cysK*, *fhuD* and *CD2992* genes increased 3.2-, 750-, 56-,  
460 12- and 10-fold, respectively, in strain 630 $\Delta$ *erm* (Fig. 5B), a result consistent with the  
461 transcriptome data (Table 3). The cysteine-dependent up-regulation of *feoB1*, *fhuD* and

462 *CD2992* was abolished in the *fur* mutant, indicating that the effect of cysteine is mediated  
463 by the Fur repressor. Interestingly, the induction of *cysK* transcription by cysteine was not  
464 completely abolished in the *fur* mutant and was only five-fold lower than it was in strain  
465 630 $\Delta$ *erm* (Fig. 5B). In addition, in the absence of cysteine, the transcript level of *cysK* was  
466 4.5-fold higher in the *fur* mutant than in strain 630 $\Delta$ *erm* (data not shown). As a Fur box is  
467 located in the promoter region of the *cysK* gene, the regulation of *cysK* by cysteine is  
468 complex, involving both direct regulation by the Fur repressor and control by a still-  
469 uncharacterized regulator. While very few data concerning the control of *cysK* expression  
470 by Fur are available (65), the cysteine-dependent regulation of CysK synthesis in *C.*  
471 *difficile* seems to be atypical.

472 The induction of the Fur regulon by cysteine suggests that the presence of cysteine in the  
473 growth medium mimics the conditions of iron depletion. A black precipitate appears  
474 when strain 630 $\Delta$ *erm* is grown in PYC (Fig. 5C). This finding is consistent with the  
475 production of high levels of H<sub>2</sub>S via cysteine degradation by cysteine desulhydrases (Fig.  
476 4C), which probably leads to the formation of this black deposit from iron-sulfide  
477 precipitation. This phenomenon is often described in anaerobic waste-collection systems  
478 (66). Therefore, iron depletion due to the precipitation of iron in the presence of excess  
479 sulfide can explain the induction of the Fur-regulated genes.

#### 480 **Regulation by cysteine of carbon and energy metabolism**

481 The ability of *C. difficile* to use a wide range of carbohydrates might be important during  
482 infection. Accordingly, Antunes et al. (13) demonstrated the existence of links between  
483 carbon metabolism and toxin production. The addition of cysteine to the medium  
484 increased the expression of several genes of carbon metabolism, including genes encoding  
485 phosphotransferase systems (PTS) and genes encoding enzymes involved in the second  
486 part of glycolysis (Fig. 6A and-Table S2).

487 The expression of genes involved in the fermentation pathways of *C. difficile* was also  
488 modulated by the presence of cysteine (Fig. 6A). Thus, the expression of *ldh* and *buk*,  
489 which encode lactate dehydrogenase and one butyrate kinase, respectively, decreased,  
490 while the expression of genes encoding pyruvate formate lyases and an alcohol  
491 dehydrogenase, increased in the presence of cysteine. Surprisingly, the *bcd2* operon,  
492 which is involved in the production of butyryl-CoA from acetyl-CoA (Fig. 6A), was not  
493 differentially expressed in the transcriptome analysis. However, when we tested the effect

of cysteine on the expression of the *bcd2* and *hbd2* genes by qRT-PCR, we showed that their transcript levels decreased 5.5- and 6-fold in PYC compared to PY, respectively. This result is in agreement with the results of a proteome analysis performed in strain VPI10463 (12), showing that the production of enzymes involved in the conversion of acetyl-CoA to butyryl-CoA (Bcd2, Crt2 and Hbd) decreases when cells are grown in presence of cysteine. To evaluate the impact of cysteine on fermentation pathways, we quantified the end products of fermentation in strain 630 $\Delta$ *erm* grown over 48 h in PY or PYC by gas-liquid chromatography. The amount of lactate and butyrate was reduced four- and six-fold, respectively, in the presence of cysteine (Fig. S2) as observed in strain VPI10463 (12). This result is consistent with the down-regulation of *ldh*, *buk* and *bcd2* operon expression. After 48 h of growth, butyric acid production was high in PY, leading to a final concentration of 5 mM compared to less than 1 mM in PYC (Fig. S2). Interestingly, the addition of butyric acid to the growth medium enhances toxin production in strain VPI10463 (12). Thus, the addition of cysteine to the medium may indirectly control toxin production at least partly via its influence on butyric acid production. However, the molecular mechanisms of the regulation of toxin synthesis in response to butyric-acid availability remain to be determined.

#### Control of amino-acid metabolism by cysteine

To analyze the impact of cysteine on amino-acid metabolism, we compared the transcriptome and the pools of amino acids obtained from strain 630 $\Delta$ *erm* grown in PY or PYC. A total of 32 genes involved in peptide or amino-acid metabolism were differentially expressed under these two conditions (Table S2), while the intracellular concentration of leucine, tyrosine, alanine, valine, phenylalanine and glutamic acid was increased in the presence of cysteine (Table 4). The expression of several genes involved in peptide degradation (*CD0779*, *CD2613*, *CD2347*, *CD2173* and *CD0166*) and amino-acid uptake (*CD2612*, *CD3092* and *CD0165*) was differentially regulated when cysteine was added to the medium (Fig. 6A). In *C. difficile*, amino-acid catabolism by the Stickland reactions can be a primary source of energy when bacteria are grown with amino acids as the sole carbon and nitrogen sources (67). Stickland reactions couple the metabolism of a pair of amino acids, of which one serves as the Stickland donor (alanine, valine, leucine or isoleucine) and is oxidatively deaminated or decarboxylated to generate ATP and reducing power (NADH), and the second serves as the Stickland acceptor (glycine,

526 proline, hydroxyproline or leucine) and is reduced or reductively deaminated,  
527 regenerating NAD<sup>+</sup> from NADH (Fig. 6B). The genes encoding the glycine reductase (*grd*)  
528 and D-proline reductase (*prd*) operons, which are involved in the reduction of the  
529 Stickland acceptors glycine and proline, were induced up to 10-fold in the presence of  
530 cysteine (Fig. 6B and Table S2). Interestingly, the expression of *proC* (*CD3281*), which is  
531 involved in the conversion of ornithine into proline, and of *CD2347*, which encodes a  
532 peptidase sharing similarities with Xaa-Pro dipeptidases and potentially generates free  
533 proline for use in the Stickland reactions (67), was also increased in the presence of  
534 cysteine.

535 In strain 630 $\Delta$ *erm* grown in the presence of cysteine, we observed a substantial  
536 accumulation of alanine (Table 4), a by-product of cysteine catabolism. Indeed, cysteine is  
537 first converted into pyruvate through cysteine desulfhydrases; pyruvate is then converted  
538 into alanine by alanine aminotransferases (Fig. 6A). *CD2828*, which shares similarities  
539 with an alanine aminotransferase characterized in *E. coli* (68), is a good candidate for this  
540 activity. However, *CD2828* was repressed in PYC (Table S2). The negative control of  
541 *CD2828* expression in the presence of a high intracellular concentration of alanine might  
542 explain this down-regulation

543 Several genes involved in the biosynthesis of branched-chain amino acids (BCAAs) were  
544 also repressed by cysteine (Fig. 6A and Table S2). The expression of *ilvD* involved in the  
545 BCAAs synthesis from pyruvate and of the *leuABCD* operon, which is involved in synthesis  
546 of leucine were down-regulated 5- to 10-fold in the presence of cysteine. Interestingly, the  
547 transcription of *brnQ1*, which encodes a BCAA transporter (Fig. 6A), was also decreased in  
548 PYC. A Tbox specific to leucine (Tbox<sub>Leu</sub>) is present in the promoter region of the *leuABCD*  
549 operon and of the *leuS* gene, indicating that these genes are probably induced during  
550 leucine starvation via premature termination of transcription (56, 69). We note that *ilvD*,  
551 *leuABCD* and *brnQ1* belong to the CodY regulon, which is involved in the adaptive  
552 response to nutrient limitation (17). Thus, the increase in the concentration of valine and  
553 leucine when cysteine is added (Table 4) might lead to the repression of genes involved in  
554 BCAAs biosynthesis and uptake through their control by a Tbox<sub>Leu</sub> or by CodY. In *B.*  
555 *subtilis*, changes in the rate of endogenous isoleucine, leucine and valine synthesis  
556 modulate the expression of CodY-regulated genes (70). In addition, for *Clostridium*  
557 *sticklandii*, using amino acids as the carbon and energy sources, cysteine is one of the six

558 amino acids that is preferentially degraded, while valine, leucine and isoleucine are used  
559 later, suggesting that certain amino acids regulate the metabolism of others (71). Cysteine  
560 is also one of the three amino acids that are preferentially used by *C. difficile* (53). Our  
561 results suggest that the presence of cysteine may delay the use of other amino acids, such  
562 as BCAAs, which are known to act as co-repressors of CodY (17). Accordingly, we  
563 observed that 31 CodY-regulated genes were repressed in strain 630 $\Delta$ erm when cysteine  
564 was added (Table S2), suggesting that cysteine has an impact on CodY activity.

### 565 **Involvement of regulators in the cysteine-dependent repression of toxin** 566 **production**

567 Toxin expression may be under the control of a global regulator that is able to sense  
568 cysteine availability. Interestingly, we showed that several genes encoding regulators are  
569 regulated in response to cysteine availability. Indeed, *CD0278*, *CD1692*, *CD2023* and  
570 *CD2065* were up- or down-regulated in the presence of cysteine (Table S2). Using the  
571 ClosTron system, we inactivated *CD0278*, *CD2023* and *CD2065*, but we did not succeed in  
572 disrupting *CD1692*. Compared to the wild-type strain, toxin-gene expression was similarly  
573 repressed by cysteine in the *CD0278*, *CD2023* and *CD2065* mutants (data not shown).  
574 However, we cannot exclude the possibility that a still-unidentified regulator intervenes  
575 in this control. Alternatively, the effector of cysteine-dependent regulation might be a  
576 cysteine by-product that is accumulated during growth in PYC. To discriminate between a  
577 direct effect of cysteine and an indirect metabolic effect, we added 10 mM cysteine to the  
578 growth medium for one hour at the onset of the stationary phase. Surprisingly, under this  
579 condition limiting the catabolism of cysteine, we observed that the transcription of *tcdA*,  
580 *tcdB* and *tcdR* was increased (Fig. S3), suggesting that cysteine down-regulates toxin  
581 production through a product of cysteine degradation (see below). As changes in carbon  
582 source and amino-acid availability were observed after the growth of *C. difficile* in the  
583 presence of cysteine (Fig. S2 and Table 4), we wondered whether toxin synthesis could be  
584 controlled by the global regulators CodY or CcpA, which are known to regulate toxin-gene  
585 expression in response to the levels of the BCAAs and PTS sugars, respectively (13, 14,  
586 18). However, we showed that toxin synthesis is similarly repressed by cysteine in the  
587 *codY* or *ccpA*-mutant and wild-type strains (Fig. 7A), indicating that CodY and CcpA do not  
588 mediate the control of toxin synthesis by cysteine.

589 The Fur regulator might also be responsible for the cysteine-dependent regulation of

590 toxin synthesis. Indeed, the expression of many virulence factors in pathogenic bacteria is  
591 negatively regulated by Fur in response to iron availability (72). We showed that TcdA  
592 production is repressed by cysteine in a *fur* mutant in the same manner as the wild-type  
593 strain (Fig. 7B), indicating that Fur is not involved in the down-regulation of toxin  
594 production in PYC. This result was in agreement with the absence of the toxin genes in the  
595 Fur transcriptome, as recently defined by Ho et al. (64).

### 596 **The role of SigL in the cysteine-dependent repression of toxin production**

597 In *C. difficile* strain VPI10463, it has been proposed that several proteins induced under  
598 toxin-producing conditions (PY) might be controlled by SigL (11). The *sigL* gene encodes a  
599 sigma factor belonging to the SigL/RpoN/ $\sigma^{54}$  family, which is known to play an important  
600 role in metabolism, adaptation and virulence (73-77). To evaluate the role of SigL in the  
601 cysteine-dependent regulation of toxin synthesis, we inactivated the *sigL* gene (Fig. S1).  
602 When we compared the level of toxin produced between the *sigL* mutant and the wild-  
603 type strain 630 $\Delta$ *erm* by dot-blot analysis, we first observed that TcdA was produced at  
604 higher levels in the *sigL* mutant than in the wild-type strain when the cells were grown in  
605 PY medium (Fig. 7B). This effect might be due to decreased competition between SigL and  
606 the toxin-specific sigma factor TcdR for the core enzyme of the RNA polymerase, as  
607 already proposed for SigH (15). Surprisingly, we observed similar levels of TcdA  
608 production in the *sigL* mutant grown in PY and PYC (Fig. 7B). To determine whether SigL  
609 regulates toxin synthesis at the transcriptional level, we tested the transcription of *tcdA*,  
610 *tcdB* and *tcdR* genes in 630 $\Delta$ *erm* and *sigL* mutant strains grown in PYC by qRT-PCR. As  
611 shown in Fig. 7C, the transcript level of *tcdA*, *tcdB* and *tcdR* was approximately 25 to 50-  
612 fold higher in the *sigL* mutant compared to the wild-type strain in the presence of  
613 cysteine. Moreover, complementation of the *sigL* mutant by a wild-type copy of *sigL*  
614 partially restored the cysteine-dependent repression of TcdA production (Fig. 7B) and of  
615 PaLoc-gene transcription (Fig. 7C). These results indicate that SigL mediates the cysteine-  
616 dependent regulation of toxin-gene expression. However, using the well-conserved  
617 consensus sequence of SigL-dependent promoters (78), we did not find a SigL-type  
618 promoter upstream of *tcdA*, *tcdB* and *tcdR*, suggesting that SigL indirectly regulates the  
619 PaLoc genes, probably in response to an increase in the by-products of cysteine  
620 degradation. Indeed, using lead-acetate paper, we showed that the production of H<sub>2</sub>S via  
621 cysteine degradation was strongly reduced in the *sigL* mutant compared to strain

622 630 $\Delta$ erm (Fig. 8A) and was restored by complementation with pDIA6309. Interestingly,  
623 according to the zymogram profile obtained with the *sigL* mutant, we showed that the  
624 cysteine desulfhydrase activity of MalY ( $\alpha$  band) significantly decreased (Fig. 4D lane 4).  
625 In addition, the expression of *malY* was four-fold lower in a *sigL* mutant compared to the  
626 wild-type strain (data not shown). This finding is in agreement with the role of SigL in the  
627 control of cysteine degradation in *C. difficile*. As pyruvate is the first product of cysteine  
628 degradation, we measured the extracellular concentration of pyruvate. We observed that  
629 in strain 630 $\Delta$ erm, the pyruvate concentration increased more than two-fold when we  
630 added cysteine to the medium. However, the level of pyruvate decreased eight-fold in the  
631 *sigL* mutant compared to the wild-type strain (Fig. 8B). In addition, the *sigL* mutant strain  
632 complemented with the wild-type copy of *sigL* had a extracellular pyruvate concentration  
633 similar to that in strain 630 $\Delta$ erm (Fig. 8B).

#### 634 **Involvement of pyruvate as a signal mediating toxin-gene repression in response to** 635 **cysteine**

636 The accumulation of H<sub>2</sub>S or pyruvate resulting from cysteine degradation during growth  
637 may be the signal modulating toxin production. To test this hypothesis, we added 10 mM  
638 of either Na<sub>2</sub>S or pyruvate to the PY medium when bacteria reached the stationary growth  
639 phase and harvested the cells after one hour of exposure. The addition of pyruvate or  
640 Na<sub>2</sub>S decreased the transcription of *tcdA*, *tcdB* and *tcdR* (Fig. 9A). Interestingly, the effect  
641 of pyruvate was not abolished when we performed a similar experiment in the *sigL*  
642 mutant (Fig. S4). This finding confirms that cysteine-dependent regulation of toxin  
643 production is mainly the consequence of the products of cysteine degradation. We also  
644 tested the effect of the pyruvate by-products such as formate and acetate on Paloc-gene  
645 transcription. The addition of 10 mM formate or acetate to the growing cell for one hour  
646 did not affect the transcription of *tcdA*, *tcdB* and *tcdR* (Fig. 9B). Thus, we concluded that  
647 pyruvate and probably sulfide are metabolic signals mediating the cysteine-dependent  
648 repression of toxin production. As the down-regulation of toxin-gene expression in the  
649 presence of cysteine (Fig. 2C) is more prominent than in the presence of pyruvate or  
650 sulfide alone (Fig. 9A), it is possible that the cysteine by-products could have a combined  
651 effect on toxin production.

#### 652 **Identification of a TCS regulating toxin-gene expression in response to pyruvate**

Pyruvate is a central metabolite of bacteria, and its cellular concentration is tightly controlled. In a broad range of bacteria, including *E. coli* and *Bacillus licheniformis*, pyruvate is excreted into the medium at the end of the exponential growth phase under the conditions of overflow metabolism. This compound is further taken up and metabolized (79, 80). In *E. coli*, the two-component system (TCS) YpdA/YpdB, which is also present in *B. licheniformis* (81), reacts predominantly to the presence of exogenous pyruvate and induces the expression of *yhjX*, which encodes a transporter of the major facilitator superfamily (79). The YpdA/YpdB system probably contributes to nutrient scavenging before entry into stationary phase. In the genome of all of the *C. difficile* strains sequenced, we found a TCS (CD2602/CD2601) that is highly similar to YpdA/YpdB. Importantly, the transmembrane-receptor domain of CD2602 shares 53% identity and 79% similarity with that of the histidine kinase YpdA, suggesting a common signal for these kinases. To determine whether CD2602-CD2601 is involved in the regulation of toxin-gene expression in response to the level of exogenous pyruvate, we inactivated the *CD2602* gene in strain 630 $\Delta$ *erm* (Fig. S1). Then, we tested the effect of pyruvate on *tcdA*, *tcdB* and *tcdR* transcription in the *CD2602* mutant. The temporary addition of pyruvate during the growth of the *CD2602* mutant had a less pronounced effect on toxin-gene transcription than it had in the wild-type strain (Fig. 9C). This result suggests that the transcriptional regulation of *tcdA*, *tcdB* and *tcdR* in response to pyruvate availability is, at least in part, mediated by the TCS CD2602-CD2601.

## Conclusion

Addition of cysteine to PY medium leads to dramatic changes in the pattern of expression of *C. difficile* genes involved in several processes, including sulfur and iron metabolism, fermentation and the stress response. These effects on gene transcription are probably related to modifications of the metabolite pools, as we showed for the repression of toxin production by metabolic changes due to cysteine degradation and transcriptional control by cysteine through a still-uncharacterized regulator. We identified SigL as a major regulator of cysteine-dependent repression of *C. difficile* toxin production. We found that the level of H<sub>2</sub>S and pyruvate resulting from cysteine degradation by cysteine desulfhydrases (32) was decreased in a *sigL* mutant, which no longer repressed toxin genes in the presence of cysteine. A similar regulation of toxin production through the metabolic conversion of cysteine to sulfate and pyruvate has been observed in *B. pertussis*

(21). SigL also seems to play an important role in the control of pyruvate metabolism in *L. monocytogenes* (82), as observed in *C. difficile* with a drop in the pyruvate concentration in the *sigL* mutant. Among the cysteine by-products produced in *C. difficile*, we demonstrated that the addition of pyruvate or H<sub>2</sub>S to PY is sufficient to repress toxin-gene expression, suggesting that pyruvate and H<sub>2</sub>S, rather than cysteine, must be metabolic signals regulating toxin production. Interestingly, when strain 630 $\Delta$ *erm* grows in the presence of cysteine, genes involved in the synthesis of pyruvate from glucose or cysteine are up-regulated, while genes required for pyruvate dissimilation leading to butyrate (*buk* operon) and lactate (*ldh*) production or involved in the biosynthesis of amino acids or fatty acids from pyruvate and acetyl-CoA, respectively, are down-regulated (Fig. 6). This change leads to the accumulation of pyruvate in the extracellular medium (Fig7B), where it is probably sensed by the membrane-associated kinase CD2602. Thus, in response to pyruvate, the response regulator CD2601 might negatively control toxin-gene expression, either directly or indirectly. Conversely, butyrate, which is known to positively regulate toxin expression (12), is found at a lower concentration in the extracellular medium (Fig. S2), which no longer stimulates toxin synthesis. Recently, it has been shown that *C. difficile* can grow in all parts of the intestinal tract of a mouse model, while toxins are only produced in the caecum and colon (83). Thus, according to the metabolites present in the small intestine and in the colon, toxin genes might be differentially expressed in the gut. Accordingly, formate and acetate (directly obtained from pyruvate) predominate in the small intestine, while the levels of propionate and butyrate are higher in the colon (84). Such a control has been described in *Salmonella typhimurium*; formate acts as a diffusible signal to induce the expression of invasion genes in the small intestine, the site that is preferentially colonized by this enteropathogen, while butyrate is present at higher concentration in the colon and repress these genes (85, 86). It is tempting to speculate that the high level of pyruvate in the small intestine represses the expression of *C. difficile* toxin genes, while butyrate mainly present in the colon induces toxin synthesis. Further biochemical studies will be necessary to characterize the signal-transduction pathway of the CD2602-CD2601 TCS. Thus, the ability of *C. difficile* to monitor the pyruvate level to adapt its physiology, metabolism and virulence might be crucial to the success of a CDI.

## Acknowledgments

This work was supported by funding from the “Institut Pasteur”. M. Dancer-Thibonnier and T. Dubois are post-doctoral fellows from the PTR program funded by the Institut Pasteur (PTR256) and the French region Ile-de-France (DIM-Malinf), respectively. The authors thank Dr. Philippe Bouvet for his help with the CPG analysis and Dr. Roselyne Garnotel and Sophie Roulin for the intracellular amino-acid content assays.

## References

1. **Freeman J, Bauer MP, Baines SD, Corver J, Fawley WN, Goorhuis B, Kuijper EJ, Wilcox MH.** 2010. The changing epidemiology of *Clostridium difficile* infections. *Clin Microbiol Rev* **23**:529-549.
2. **Carter GP, Douce GR, Govind R, Howarth PM, Mackin KE, Spencer J, Buckley AM, Antunes A, Kotsanas D, Jenkin GA, Dupuy B, Rood JI, Lyras D.** 2011. The anti-sigma factor TcdC modulates hypervirulence in an epidemic BI/NAP1/027 clinical isolate of *Clostridium difficile*. *PLoS Pathog* **7**:e1002317.
3. **Mani N, Dupuy B.** 2001. Regulation of toxin synthesis in *Clostridium difficile* by an alternative RNA polymerase sigma factor. *Proceedings of the National Academy of Sciences of the United States of America* **98**:5844-5849.
4. **Matamouros S, England P, Dupuy B.** 2007. *Clostridium difficile* toxin expression is inhibited by the novel regulator TcdC. *Mol Microbiol* **64**:1274-1288.
5. **Govind R, Dupuy B.** 2012. Secretion of *Clostridium difficile* toxins A and B requires the holin-like protein TcdE. *PLoS Pathog* **8**:e1002727.
6. **Akerlund T, Svenungsson B, Lagergren A, Burman LG.** 2006. Correlation of disease severity with fecal toxin levels in patients with *Clostridium difficile*-associated diarrhea and distribution of PCR ribotypes and toxin yields in vitro of corresponding isolates. *J Clin Microbiol* **44**:353-358.
7. **Dupuy B, Sonenshein AL.** 1998. Regulated transcription of *Clostridium difficile* toxin genes. *Molecular Microbiology* **27**:107-120.
8. **Karlsson S, Dupuy B, Mukherjee K, Norin E, Burman LG, Akerlund T.** 2003. Expression of *Clostridium difficile* toxins A and B and their sigma factor TcdD is controlled by temperature. *Infection and Immunity* **71**:1784-1793.
9. **Deneve C, Delomenie C, Barc MC, Collignon A, Janoir C.** 2008. Antibiotics involved in *Clostridium difficile*-associated disease increase colonization factor gene expression. *J Med Microbiol* **57**:732-738.
10. **Bouillaut L, Self WT, Sonenshein AL.** 2013. Proline-dependent regulation of *Clostridium difficile* Stickland metabolism. *J Bacteriol* **195**:844-854.
11. **Karlsson S, Burman LG, Akerlund T.** 2008. Induction of toxins in *Clostridium difficile* is associated with dramatic changes of its metabolism. *Microbiology* **154**:3430-3436.
12. **Karlsson S, Lindberg A, Norin E, Burman LG, Akerlund T.** 2000. Toxins, Butyric Acid, and Other Short-Chain Fatty Acids Are Coordinately Expressed and Down-Regulated by Cysteine in *Clostridium difficile*. *Infection and Immunity* **68**:5881-5888.

- 761 13. **Antunes A, Martin-Verstraete I, Dupuy B.** 2011. CcpA mediated repression of  
762 *Clostridium difficile* toxin gene expression. Mol Microbiol **in press**.
- 763 14. **Dineen SS, Villapakkam AC, Nordman JT, Sonenshein AL.** 2007. Repression of  
764 *Clostridium difficile* toxin gene expression by CodY. Mol Microbiol **66**:206-219.
- 765 15. **Saujet L, Monot M, Dupuy B, Soutourina O, Martin-Verstraete I.** 2011. The key  
766 sigma factor of transition phase, SigH, controls sporulation, metabolism and  
767 virulence factor expression in *Clostridium difficile*. J Bacteriol doi:JB.00272-11  
768 [pii]10.1128/JB.00272-11.
- 769 16. **Underwood S, Guan S, Vijayasubhash V, Baines SD, Graham L, Lewis RJ,**  
770 **Wilcox MH, Stephenson K.** 2009. Characterization of the sporulation initiation  
771 pathway of *Clostridium difficile* and its role in toxin production. J Bacteriol  
772 **191**:7296-7305.
- 773 17. **Dineen SS, McBride SM, Sonenshein AL.** 2010. Integration of metabolism and  
774 virulence by *Clostridium difficile* CodY. J Bacteriol **192**:5350-5362.
- 775 18. **Antunes A, Camiade E, Monot M, Courtois E, Barbut F, Sernova NV, Rodionov**  
776 **DA, Martin-Verstraete I, Dupuy B.** 2012. Global transcriptional control by  
777 glucose and carbon regulator CcpA in *Clostridium difficile*. Nucleic Acids Res  
778 **40**:10701-10718.
- 779 19. **Theriot CM, Koenigsnecht MJ, Carlson PE, Jr., Hatton GE, Nelson AM, Li B,**  
780 **Huffnagle GB, J ZL, Young VB.** 2014. Antibiotic-induced shifts in the mouse gut  
781 microbiome and metabolome increase susceptibility to *Clostridium difficile*  
782 infection. Nat Commun **5**:3114.
- 783 20. **Andre G, Haudecoeur E, Monot M, Ohtani K, Shimizu T, Dupuy B, Martin-**  
784 **Verstraete I.** 2010. Global regulation of gene expression in response to cysteine  
785 availability in *Clostridium perfringens*. BMC Microbiol **10**:234.
- 786 21. **Bogdan JA, Nazario-Larrieu J, Sarwar J, Alexander P, Blake MS.** 2001.  
787 *Bordetella pertussis* autoregulates pertussis toxin production through the  
788 metabolism of cysteine. Infect Immun **69**:6823-6830.
- 789 22. **Grifantini R, Bartolini E, Muzzi A, Draghi M, Frigimelica E, Berger J,**  
790 **Randazzo F, Grandi G.** 2002. Gene expression profile in *Neisseria meningitidis*  
791 and *Neisseria lactamica* upon host-cell contact: from basic research to vaccine  
792 development. Ann NY Acad Sci **975**:202-216.
- 793 23. **Hatzios SK, Bertozzi CR.** 2011. The regulation of sulfur metabolism in  
794 *Mycobacterium tuberculosis*. PLoS Pathog **7**:e1002036.
- 795 24. **Mendez J, Reimundo P, Perez-Pascual D, Navais R, Gomez E, Guijarro JA.**  
796 2011. A novel *cdsAB* operon is involved in the uptake of L-cysteine and  
797 participates in the pathogenesis of *Yersinia ruckeri*. J Bacteriol **193**:944-951.
- 798 25. **Shelver D, Rajagopal L, Harris TO, Rubens CE.** 2003. MtaR, a regulator of  
799 methionine transport, is critical for survival of group B streptococcus in vivo. J  
800 Bacteriol **185**:6592-6599.
- 801 26. **Xayarath B, Marquis H, Port GC, Freitag NE.** 2009. *Listeria monocytogenes*  
802 CtaP is a multifunctional cysteine transport-associated protein required for  
803 bacterial pathogenesis. Mol Microbiol **74**:956-973.
- 804 27. **Soutourina O, Dubrac S, Poupel O, Msadek T, Martin-Verstraete I.** 2010. The  
805 pleiotropic CymR regulator of *Staphylococcus aureus* plays an important role in  
806 virulence and stress response. PLoS Pathog **6**:e1000894.
- 807 28. **Masip L, Veeravalli K, Georgiou G.** 2006. The many faces of glutathione in  
808 bacteria. Antioxid Redox Signal **8**:753-762.

- 809 29. **Zeller T, Klug G.** 2006. Thioredoxins in bacteria: functions in oxidative stress  
810 response and regulation of thioredoxin genes. *Naturwissenschaften* **93**:259-266.
- 811 30. **Guédon E, Martin-Verstraete I.** 2007. Cysteine metabolism and its regulation in  
812 bacteria, p 195-218. *In* Wendisch VF (ed), *Amino acid biosynthesis-pathways,*  
813 *regulation and metabolic engineering.* Springer.
- 814 31. **Hullo MF, Auger S, Soutourina O, Barzu O, Yvon M, Danchin A, Martin-**  
815 **Verstraete I.** 2007. Conversion of methionine to cysteine in *Bacillus subtilis* and  
816 its regulation. *J Bacteriol* **189**:187-197.
- 817 32. **Auger S, Gomez MP, Danchin A, Martin-Verstraete I.** 2005. The PatB protein of  
818 *Bacillus subtilis* is a C-S-lyase. *Biochimie* **87**:231-238.
- 819 33. **Gutierrez-Preciado A, Henkin TM, Grundy FJ, Yanofsky C, Merino E.** 2009.  
820 Biochemical features and functional implications of the RNA-based T-box  
821 regulatory mechanism. *Microbiol Mol Biol Rev* **73**:36-61.
- 822 34. **Even S, Burguière P, Auger S, Soutourina O, Danchin A, Martin-Verstraete I.**  
823 2006. Global control of cysteine metabolism by CymR in *Bacillus subtilis*. *J*  
824 *Bacteriol* **188**:2184-2197.
- 825 35. **Soutourina O, Poupel O, Coppee JY, Danchin A, Msadek T, Martin-Verstraete**  
826 **I.** 2009. CymR, the master regulator of cysteine metabolism in *Staphylococcus*  
827 *aureus*, controls host sulfur source utilization and plays a role in biofilm  
828 formation. *Mol Microbiol* **73**:194-211.
- 829 36. **Fagan RP, Fairweather NF.** 2011. *Clostridium difficile* has two parallel and  
830 essential Sec secretion systems. *J Biol Chem* **286**:27483-27493.
- 831 37. **Lopez del Castillo Lozano M, Tache R, Bonnarme P, Landaud S.** 2007.  
832 Evaluation of a quantitative screening method for hydrogen sulfide production  
833 by cheese-ripening microorganisms: the first step towards l-cysteine catabolism.  
834 *J Microbiol Methods* **69**:70-77.
- 835 38. **Tanous C, Soutourina O, Raynal B, Hullo MF, Mervelet P, Gilles AM, Noirot P,**  
836 **Danchin A, England P, Martin-Verstraete I.** 2008. The CymR Regulator in  
837 Complex with the Enzyme CysK Controls Cysteine Metabolism in *Bacillus subtilis*.  
838 *J Biol Chem* **283**:35551-35560.
- 839 39. **Heap JT, Pennington OJ, Cartman ST, Carter GP, Minton NP.** 2007. The  
840 Clostron: A universal gene knock-out system for the genus *Clostridium*. *J*  
841 *Microbiol Methods* **70**:452-464.
- 842 40. **Heap JT, Pennington OJ, Cartman ST, Minton NP.** 2009. A modular system for  
843 *Clostridium* shuttle plasmids. *J Microbiol Methods* **78**:79-85.
- 844 41. **Livak KJ, Schmittgen TD.** 2001. Analysis of relative gene expression data using  
845 real-time quantitative PCR and the 2(-Delta Delta C(T)) Method. *Methods*  
846 **25**:402-408.
- 847 42. **Breitling R, Armengaud P, Amtmann A, Herzyk P.** 2004. Rank products: a  
848 simple, yet powerful, new method to detect differentially regulated genes in  
849 replicated microarray experiments. *FEBS Lett* **573**:83-92.
- 850 43. **Smyth GK, Speed T.** 2003. Normalization of cDNA microarray data. *Methods*  
851 **31**:265-273.
- 852 44. **Benjamini Y, Hochberg Y.** 1995. Controlling the false discovery rate: a practical  
853 and powerful approach to multiple testing. *J Roy Statist Soc Ser*:289--300.
- 854 45. **Sebaihia M, Wren BW, Mullany P, Fairweather NF, Minton N, Stabler R,**  
855 **Thomson NR, Roberts AP, Cerdeno-Tarraga AM, Wang H, Holden MT, Wright**  
856 **A, Churcher C, Quail MA, Baker S, Bason N, Brooks K, Chillingworth T,**  
857 **Cronin A, Davis P, Dowd L, Fraser A, Feltwell T, Hance Z, Holroyd S, Jagels K,**

- 858 **Moule S, Mungall K, Price C, Rabbino-witsch E, Sharp S, Simmonds M, Stevens**  
859 **K, Unwin L, Whithead S, Dupuy B, Dougan G, Barrell B, Parkhill J.** 2006. The  
860 multidrug-resistant human pathogen *Clostridium difficile* has a highly mobile,  
861 mosaic genome. *Nat Genet* **38**:779-786.
- 862 46. **Mehta PK, Christen P.** 2000. The molecular evolution of pyridoxal-5'-phosphate-  
863 dependent enzymes. *Adv Enzymol Relat Areas Mol Biol* **74**:129-184.
- 864 47. **Andre G, Even S, Putzer H, Burguiere P, Croux C, Danchin A, Martin-**  
865 **Verstraete I, Soutourina O.** 2008. S-box and T-box riboswitches and antisense  
866 RNA control a sulfur metabolic operon of *Clostridium acetobutylicum*. *Nucleic*  
867 *Acids Res* **36**:5955-5969.
- 868 48. **Manukhov IV, Mamaeva DV, Rastorguev SM, Faleev NG, Morozova EA,**  
869 **Demidkina TV, Zavilgelsky GB.** 2005. A gene encoding L-methionine gamma-  
870 lyase is present in Enterobacteriaceae family genomes: identification and  
871 characterization of *Citrobacter freundii* L-methionine gamma-lyase. *J Bacteriol*  
872 **187**:3889-3893.
- 873 49. **Dias B, Weimer B.** 1998. Purification and characterization of L-methionine  
874 gamma-lyase from *Brevibacterium linens* BL2. *Appl Environ Microbiol* **64**:3327-  
875 3331.
- 876 50. **Ali V, Nozaki T.** 2007. Current therapeutics, their problems, and sulfur-  
877 containing-amino-acid metabolism as a novel target against infections by  
878 "amitochondriate" protozoan parasites. *Clin Microbiol Rev* **20**:164-187.
- 879 51. **Dembek M, Barquist L, Boinett CJ, Cain AK, Mayho M, Lawley TD,**  
880 **Fairweather NF, Fagan RP.** 2015. High-throughput analysis of gene essentiality  
881 and sporulation in *Clostridium difficile*. *MBio* **6**:e02383.
- 882 52. **Boudry P, Gracia C, Monot M, Caillet J, Saujet L, Hajnsdorf E, Dupuy B,**  
883 **Martin-Verstraete I, Soutourina O.** 2014. Pleiotropic role of the RNA chaperone  
884 protein Hfq in the human pathogen *Clostridium difficile*. *J Bacteriol* **196**:3234-  
885 3248.
- 886 53. **Neumann-Schaal M, Hofmann JD, Will SE, Schomburg D.** 2015. Time-resolved  
887 amino acid uptake of *Clostridium difficile* 630Deltaerm and concomitant  
888 fermentation product and toxin formation. *BMC Microbiol* **15**:281.
- 889 54. **Hullo MF, Auger S, Dassa E, Danchin A, Martin-Verstraete I.** 2004. The  
890 *metNPQ* operon of *Bacillus subtilis* encodes an ABC permease transporting  
891 methionine sulfoxide, D- and L-methionine. *Res Microbiol* **155**:80-86.
- 892 55. **Rodionov DA, Vitreschak AG, Mironov AA, Gelfand MS.** 2004. Comparative  
893 genomics of the methionine metabolism in Gram-positive bacteria: a variety of  
894 regulatory systems. *Nucleic Acids Research* **32**:3340-3353.
- 895 56. **Soutourina OA, Monot M, Boudry P, Saujet L, Pichon C, Sismeiro O,**  
896 **Semenova E, Severinov K, Le Bouguenec C, Coppee JY, Dupuy B, Martin-**  
897 **Verstraete I.** 2013. Genome-Wide Identification of Regulatory RNAs in the  
898 Human Pathogen *Clostridium difficile*. *PLoS Genet* **9**:e1003493.
- 899 57. **Burguiere P, Auger S, Hullo MF, Danchin A, Martin-Verstraete I.** 2004. Three  
900 different systems participate in L-cystine uptake in *Bacillus subtilis*. *J Bacteriol*  
901 **186**:4875-4884.
- 902 58. **Awano N, Wada M, Mori H, Nakamori S, Takagi H.** 2005. Identification and  
903 functional analysis of *Escherichia coli* cysteine desulhydrases. *Appl Environ*  
904 *Microbiol* **71**:4149-4152.
- 905 59. **Hindson VJ.** 2003. Serine acetyltransferase of *Escherichia coli*: substrate  
906 specificity and feedback control by cysteine. *Biochem J* **375**:745-752.

- 907 60. **Harris CL.** 1981. Cysteine and growth inhibition of *Escherichia coli*: threonine  
908 deaminase as the target enzyme. *J Bacteriol* **145**:1031-1035.
- 909 61. **Lee JW, Helmann JD.** 2007. Functional specialization within the Fur family of  
910 metalloregulators. *Biometals* **20**:485-499.
- 911 62. **Vasileva D, Janssen H, Honicke D, Ehrenreich A, Bahl H.** 2012. Effect of iron  
912 limitation and fur gene inactivation on the transcriptional profile of the strict  
913 anaerobe *Clostridium acetobutylicum*. *Microbiology* **158**:1918-1929.
- 914 63. **Ollinger J, Song KB, Antelmann H, Hecker M, Helmann JD.** 2006. Role of the  
915 Fur regulon in iron transport in *Bacillus subtilis*. *J Bacteriol* **188**:3664-3673.
- 916 64. **Ho TD, Ellermeier CD.** 2015. Ferric Uptake Regulator Fur Control of Putative  
917 Iron Acquisition Systems in *Clostridium difficile*. *J Bacteriol* **197**:2930-2940.
- 918 65. **Torres VJ, Attia AS, Mason WJ, Hood MI, Corbin BD, Beasley FC, Anderson  
919 KL, Stauff DL, McDonald WH, Zimmerman LJ, Friedman DB, Heinrichs DE,  
920 Dunman PM, Skaar EP.** 2010. *Staphylococcus aureus* fur regulates the  
921 expression of virulence factors that contribute to the pathogenesis of pneumonia.  
922 *Infect Immun* **78**:1618-1628.
- 923 66. **Nielsen AH, Hvitved-Jacobsen T, Vollertsen J.** 2008. Effects of pH and iron  
924 concentrations on sulfide precipitation in wastewater collection systems. *Water  
925 Environ Res* **80**:380-384.
- 926 67. **Jackson S, Calos M, Myers A, Self WT.** 2006. Analysis of proline reduction in the  
927 nosocomial pathogen *Clostridium difficile*. *J Bacteriol* **188**:8487-8495.
- 928 68. **Kim SH, Schneider BL, Reitzer L.** 2010. Genetics and regulation of the major  
929 enzymes of alanine synthesis in *Escherichia coli*. *J Bacteriol* **192**:5304-5311.
- 930 69. **Vitreschak AG, Mironov AA, Lyubetsky VA, Gelfand MS.** 2008. Comparative  
931 genomic analysis of T-box regulatory systems in bacteria. *RNA* **14**:717-735.
- 932 70. **Brinsmade SR, Kleijn RJ, Sauer U, Sonenshein AL.** 2010. Regulation of CodY  
933 activity through modulation of intracellular branched-chain amino acid pools. *J  
934 Bacteriol* **192**:6357-6368.
- 935 71. **Fonknechten N, Chaussonnerie S, Tricot S, Lajus A, Andreesen JR, Perchat N,  
936 Pelletier E, Gouyvenoux M, Barbe V, Salanoubat M, Le Paslier D,  
937 Weissenbach J, Cohen GN, Kreimeyer A.** 2010. *Clostridium sticklandii*, a  
938 specialist in amino acid degradation: revisiting its metabolism through its genome  
939 sequence. *BMC Genomics* **11**:555.
- 940 72. **Troxell B, Hassan HM.** 2013. Transcriptional regulation by Ferric Uptake  
941 Regulator (Fur) in pathogenic bacteria. *Front Cell Infect Microbiol* **3**:59.
- 942 73. **Dalet K, Briand C, Cenatiempo Y, Hechard Y.** 2000. The rpoN gene of  
943 *Enterococcus faecalis* directs sensitivity to subclass IIa bacteriocins. *Curr  
944 Microbiol* **41**:441-443.
- 945 74. **Iyer VS, Hancock LE.** 2012. Deletion of sigma(54) (rpoN) alters the rate of  
946 autolysis and biofilm formation in *Enterococcus faecalis*. *J Bacteriol* **194**:368-  
947 375.
- 948 75. **Mattila M, Somervuo P, Rattei T, Korkeala H, Stephan R, Tasara T.** 2012.  
949 Phenotypic and transcriptomic analyses of Sigma L-dependent characteristics in  
950 *Listeria monocytogenes* EGD-e. *Food Microbiol* **32**:152-164.
- 951 76. **Okada Y, Okada N, Makino S, Asakura H, Yamamoto S, Igimi S.** 2006. The  
952 sigma factor RpoN (sigma54) is involved in osmotolerance in *Listeria  
953 monocytogenes*. *FEMS Microbiol Lett* **263**:54-60.

- 954 77. **Saldias MS, Lamothe J, Wu R, Valvano MA.** 2008. Burkholderia cenocepacia  
955 requires the RpoN sigma factor for biofilm formation and intracellular trafficking  
956 within macrophages. *Infect Immun* **76**:1059-1067.
- 957 78. **Francke C, Groot Kormelink T, Hagemeijer Y, Overmars L, Sluijter V,**  
958 **Moezelaar R, Siezen RJ.** 2011. Comparative analyses imply that the enigmatic  
959 Sigma factor 54 is a central controller of the bacterial exterior. *BMC Genomics*  
960 **12**:385.
- 961 79. **Fried L, Behr S, Jung K.** 2013. Identification of a target gene and activating  
962 stimulus for the YpdA/YpdB histidine kinase/response regulator system in  
963 Escherichia coli. *J Bacteriol* **195**:807-815.
- 964 80. **Paczia N, Nilgen A, Lehmann T, Gatgens J, Wiechert W, Noack S.** 2012.  
965 Extensive exometabolome analysis reveals extended overflow metabolism in  
966 various microorganisms. *Microb Cell Fact* **11**:122.
- 967 81. **Yangtse W, Zhou Y, Lei Y, Qiu Y, Wei X, Ji Z, Qi G, Yong Y, Chen L, Chen S.** 2012.  
968 Genome sequence of Bacillus licheniformis WX-02. *J Bacteriol* **194**:3561-3562.
- 969 82. **Arous S, Buchrieser C, Folio P, Glaser P, Namane A, Hebraud M, Hechard Y.**  
970 2004. Global analysis of gene expression in an rpoN mutant of Listeria  
971 monocytogenes. *Microbiology* **150**:1581-1590.
- 972 83. **Koenigsknecht MJ, Theriot CM, Bergin IL, Schumacher CA, Schloss PD, Young**  
973 **VB.** 2015. Dynamics and establishment of Clostridium difficile infection in the  
974 murine gastrointestinal tract. *Infect Immun* **83**:934-941.
- 975 84. **Keeney KM, Finlay BB.** 2011. Enteric pathogen exploitation of the microbiota-  
976 generated nutrient environment of the gut. *Curr Opin Microbiol* **14**:92-98.
- 977 85. **Gantois I, Ducatelle R, Pasmans F, Haesebrouck F, Hautefort I, Thompson A,**  
978 **Hinton JC, Van Immerseel F.** 2006. Butyrate specifically down-regulates  
979 salmonella pathogenicity island 1 gene expression. *Appl Environ Microbiol*  
980 **72**:946-949.
- 981 86. **Huang Y, Suyemoto M, Garner CD, Cicconi KM, Altier C.** 2008. Formate acts as  
982 a diffusible signal to induce Salmonella invasion. *J Bacteriol* **190**:4233-4241.
- 983 87. **Hussain, H.A, A.P, Robert and P. Mullany** Generation of an erythromycin-  
984 sensitive derivative of Clostridium difficile strain 630 (630Deltaerm) and  
985 demonstration that the conjugative transposon Tn916DeltaE enters the genome of  
986 this strain at multiple sites. *J Med Microbiol.* **54**:137-41.
- 987 88. **O'Connor, J. R., D. Lyras, K. A. Farrow, V. Adams, D. R. Powell, J. Hinds, J. K.**  
988 **Cheung, and J. I. Rood.** 2006. Construction and analysis of chromosomal  
989 *Clostridium difficile* mutants. *Mol. Microbiol.* **61**:1335-1351.
- 990  
991  
992  
993  
994

995 **Tables and figures**

996  
997 **Figure 1. Schematic overview of sulfur metabolism in bacteria**

998 APS, adenylyl sulfate; OAS, *O*-acetylserine; OAH, *O*-acetylhomoserine; SAM, S-adenosyl-  
999 methionine.

1000  
1001 **Figure 2. Effect of cysteine on toxin production in different *C. difficile* strains**

1002 A) Cytotoxicity assays on Vero cells. Two-fold serial dilutions of intracellular bacterial  
1003 crude extracts were performed, and the dilutions were added to a 96-well plate of  
1004 confluent Vero cells. The toxin titer corresponds to the lowest dilution of *C. difficile* crude  
1005 extracts required for > 50 % cell rounding. Cytotoxicity results are presented as the ratio  
1006 of the toxin titers of bacterial cells grown in the presence of cysteine (PYC) to those of  
1007 bacterial cells grown in the absence of cysteine (PY). B) TcdA dot-blot analysis. The crude  
1008 extracts of *C. difficile* strains (200 ng for strains 630 $\Delta$ erm, M7404 and M7404  
1009 complemented with pDLL17-*tcdC* and 20 ng for strain VPI10463) were probed with anti-  
1010 TcdA antibodies as described in the materials and methods section. The results presented  
1011 are representative of crude extracts tested from at least three independent experiments.  
1012 C) Transcript levels of *tcdR*, *tcdA* and *tcdB* genes in strain 630 $\Delta$ erm grown in the presence  
1013 or absence of cysteine. . results are presented as the ratio of the mRNA level (arbitrary  
1014 units) of each gene in bacterial cells grown in the presence of cysteine (PYC) to that of  
1015 each gene in cells grown in the absence (PY) of cysteine. The results are the averages of at  
1016 least three independent experiments (error bars are the standard deviations from the  
1017 mean values). The statistical analysis was performed by using a t-test (*tcdA*, *tcdR*) or a  
1018 Mann-Whitney test (*tcdB*).

1019  
1020 **Figure 3. Reconstruction of sulfur metabolism in *C. difficile***

1021 Genes of strain 630 $\Delta$ erm are renamed on the basis of *B. subtilis* orthologs. *cysE*: serine *O*-  
1022 acetyltransferase (CD1595); *cysK*: OAS-thiol-lyase (CD1594); *asrABC*: anaerobic sulfite  
1023 reductase (CD2231-2233); *ssuCBA<sub>1</sub>*: ABC-transport system sulfonates (CD1482-1484);  
1024 *ssuCBA<sub>2</sub>*: ABC-transport system sulfonates (CD2989-2991); *metA*: homoserine acetyl-  
1025 transferase (CD1826); *metY*: OAH thiol-lyase (CD1825); *maly*: cystathionine  $\beta$ -lyase  
1026 (CD3029); *metH*: cobalamin-dependent methionine synthase (CD3596); *metK*: SAM  
1027 synthetase (CD0130); *mtnN*: adenosylhomocysteine nucleosidase (CD2611); *luxS*: S-  
1028 ribosylhomocysteine lyase (CD3598); *mdeA*: methionine  $\gamma$ -lyase (CD3577), *metNIQ<sub>1</sub>*: ABC-

1029 transport system methionine (CD1489-1491); *pepT*, peptidase T (CD1046); *pepA*, leucine  
1030 aminopeptidase (CD1300); AI-2, autoinducer 2; OAS; *O*-acetylserine; OAH, *O*-  
1031 acetylhomoserine SAM, S-adenosyl-methionine; SAH, S-adenosyl-homocysteine; SRH, S-  
1032 ribosyl-homocysteine. Ext means "external". As indicated, an S-box motif is located  
1033 upstream of the *metY-metA* and *metNIQ<sub>1</sub>* operons and of the *metQ<sub>2</sub>* and *metK* genes,  
1034 suggesting that they are controlled by a SAM-dependent riboswitch (55). A Tbox is  
1035 present upstream of *hom-CD1580*.

1036

1037 **Figure 4. Hydrogen sulfide production in strain 630 $\Delta$ erm.**

1038 A) Detection of H<sub>2</sub>S production using lead-acetate paper. H<sub>2</sub>S production was evaluated in  
1039 PY, PY plus cysteine (PYC) and PY plus homocysteine (PYHC) media. The production of  
1040 H<sub>2</sub>S yielded a black color due to the formation of PbS. B) Detection of the homocysteine g-  
1041 lyase activity on a zymogram. Crude extracts of strain 630 $\Delta$ erm grown in PY, PYC or PYHC  
1042 were loaded on a native polyacrylamide gel (12 %) and incubated with 10 mM  
1043 homocysteine. Homocysteine  $\gamma$ -lyase was detected by the formation of insoluble PbS via  
1044 the release of H<sub>2</sub>S. Lanes of the zymogram have been reorganized from the same image to  
1045 present data chronologically. C) Quantitative detection of H<sub>2</sub>S after 6 h or 10 h of growth  
1046 of strain 630 $\Delta$ erm in PY (white boxes) or PYC (black boxes). H<sub>2</sub>S production was  
1047 measured using the quantitative methylene blue method, as described in the materials  
1048 and methods section. The statistical analysis was performed by using Mann-Whitney test  
1049 for all genes. D) Detection of cysteine desulphydrase activities on a zymogram. Crude  
1050 extracts of strain 630 $\Delta$ erm (lane 1 and lane 2), 630 $\Delta$ erm::*cysK* (lane 3), 630 $\Delta$ erm::*sigL*  
1051 (lane 4), 630 $\Delta$ erm + pRPF185 (lane 5) and 630 $\Delta$ erm + pDIA6456-AS*malY* (lane 6). The  
1052 strains were grown in PY (lane 1) or PYC (lane 2 to 6). Samples were charged on a native  
1053 polyacrylamide gel (12 %) and incubated with 10 mM cysteine. The cysteine  
1054 desulphydrases were detected by the formation of insoluble PbS formed by the release of  
1055 H<sub>2</sub>S. The results presented are representative of at least three independent experiments.  
1056 Lanes of the zymogram have been reorganized from the same image to present data  
1057 chronologically

1058

1059 **Figure 5. Analysis of Fur-regulated genes induced in the presence of cysteine**

1060 A) Consensus sequence of the Fur box motif of *C. difficile*. The sequence logo was created  
1061 by the alignment of putative Fur-regulated genes induced in the presence of cysteine on

1062 the Weblogo website (<http://weblogo.berkeley.edu>). The height of the nucleotides is  
1063 proportional to their frequencyB) Effect of cysteine on the transcript level of *fur*  
1064 (CD1287), *feoB1* (CD1479), *cysK* (CD1594), *fhuD* (CD2878) and *CD2992* in *630Δerm* and  
1065 the *630Δerm::fur*. The *630Δerm* (white boxes) and *630Δerm::fur* (black boxes) strains  
1066 were grown for 10 h in PY or PYC. qRT-PCR results are presented as the ratio of the  
1067 amount of mRNA (arbitrary units) of each gene in bacterial cells grown in PYC to that of  
1068 each mRNA in the bacterial cells grown in PY. Data are the averages of at least three  
1069 independent experiments (error bars are the standard deviations from the mean values).  
1070 C) Aspect of the bacterial pellet of strain *630Δerm* grown for 10 h in PY or in PYC. The  
1071 black precipitate is due to FeS precipitation.

1072

1073 **Figure 6. Overview of *C. difficile* genes involved in carbon and amino acid**  
1074 **metabolism that are differentially expressed in the presence of cysteine.** Genes that  
1075 are up- and down-regulated in the presence of cysteine in the transcriptome analysis are  
1076 indicated in red and green, respectively. "\*" means that the differential transcript level  
1077 was detected by qRT-PCR. A) Carbon metabolism and fermentation pathways.  
1078 Assignments of genes regulated by cysteine availability are as follows: *tpi*,  
1079 triosephosphate isomerase; *gapA/gapN*, glyceraldehyde-3-phosphate dehydrogenase;  
1080 *pgk*, phosphoglycerate kinase; *pgm*, 2,3-bisphosphoglycerate-mutase; *celABC*, PTS  
1081 cellobiose; *celF*, cellobiose-6-P hydrolase; *ldh*, lactate dehydrogenase; *adhE*, aldehyde-  
1082 alcohol dehydrogenase; *pflB* and *pflD*, pyruvate formate lyase; *pflE* and *pflA*, pyruvate  
1083 formate lyase activating enzyme; *thiA1*, acetyl-CoA acetyltransferase; *bcd2*, butyryl-CoA  
1084 dehydrogenase; *hbD2*, 3-hydroxybutyryl-CoA dehydrogenase; *crt2*, 3-hydroxybutyryl-CoA  
1085 dehydratase; *buk*, butyrate kinase; *malY*, cysteine desulfhydrase; *ilvD*, dihydroxy-acid  
1086 dehydratase; *leuA*, 2-isopropylmalate synthase; *leuB*, 3-isopropylmalate dehydrogenase;  
1087 *leuC*, 3-isopropylmalate dehydratase large subunit; *leuD*, 3-isopropylmalate dehydratase  
1088 small subunit; *brnQ1*, BCAA transporter. B) Stickland reactions and associated  
1089 metabolism. Assignments of genes regulated in response to cysteine availability are as  
1090 follows: *grdDCBAEX*, glycine reductase complex; *prdEDBA*, proline reductase; *prdF*,  
1091 proline racemase; *CD2347*, putative Xaa-Pro dipeptidase; *proC*, pyrroline-5-carboxylate  
1092 reductase, *gcvPB*, glycine decarboxylase; *gcvTPA*, bi-functional glycine  
1093 dehydrogenase/aminomethyl transferase protein.

1094

1095 **Figure 7. Role of Fur, CcpA, CodY and SigL in the cysteine-dependent repression of**  
1096 **toxin production.** Strains JIR8094, JIR8094::*codY* and JIR8094::*ccpA* (A) and strains  
1097 630 $\Delta$ *erm*, 630 $\Delta$ *erm*::*fur*, 630 $\Delta$ *erm*::*sigL* and 630 $\Delta$ *erm*::*sigL* + pDIA6309-*sigL* (B) were  
1098 grown for 10 h in PY or PYC. TcdA production was estimated from crude extracts by dot-  
1099 blot analysis using an anti-TcdA antibody. The results are representative of at least three  
1100 independent experiments. C) Effect of cysteine on *tcdA*, *tcdB* and *tcdR* transcript levels in  
1101 630 $\Delta$ *erm*::*sigL* (white boxes) or 630 $\Delta$ *erm*::*sigL* complemented with pDIA6309-*sigL* (black  
1102 boxes) versus the wild-type strain 630 $\Delta$ *erm*. All strains were grown for 10 h in PYC. qRT-  
1103 PCR results are presented as the ratio between the amount of the mRNA (arbitrary units)  
1104 of each gene normalized by the DNA *polIII* gene in both 630 $\Delta$ *erm*::*sigL* and 630 $\Delta$ *erm*::*sigL*  
1105 complemented with pDIA6309-*sigL* compared to the mRNA level in the wild-type strain.  
1106 Data are the averages of at least three independent experiments (error bars are the  
1107 standard deviations from the mean values). The statistical analysis was performed by  
1108 using a t-test for all genes with an exception for *tcdB* (Mann-Whitney test).

1109

1110 **Figure 8. Effect of *sigL* inactivation on cysteine degradation and pyruvate**  
1111 **production**

1112 A) Detection of H<sub>2</sub>S production in the 630 $\Delta$ *erm*, 630 $\Delta$ *erm*::*sigL* and 630 $\Delta$ *erm*::*sigL* +  
1113 pDIA6309-*sigL* strains grown in PYC by using lead-acetate papers. B) Quantitative  
1114 detection of pyruvate in the supernatant of strains 630 $\Delta$ *erm*, 630 $\Delta$ *erm*::*sigL* and  
1115 630 $\Delta$ *erm*::*sigL* + pDIA6309-*sigL* after 10 h of growth in PY (white boxes) or PYC (black  
1116 boxes). The statistical analysis was performed by using Mann-Whitney test for all genes,  
1117 ns: non significant.

1118

1119 **Figure 9. Effect of pyruvate and Na<sub>2</sub>S on toxin-gene expression**

1120 A) Transcript levels of *tcdA*, *tcdB* and *tcdR* genes in strain 630 $\Delta$ *erm* after 1 h of exposure  
1121 to pyruvate (white boxes) or Na<sub>2</sub>S (black boxes). The strain was grown in PY for 9 h, and  
1122 10 mM pyruvate or 10 mM Na<sub>2</sub>S was then added to the medium. Cells were centrifuged 1  
1123 h later. The statistical analysis was performed by using a t-test for all genes, with an  
1124 exception for *tcdB*+Na<sub>2</sub>S (Mann-Whitney test). B) Transcript levels of the *tcdA*, *tcdB* and  
1125 *tcdR* genes of strain 630 $\Delta$ *erm* after 1 h of exposure to formate (white boxes) or acetate  
1126 (black boxes). The strain was grown in PY for 9 h and 10 mM formate or 10 mM acetate  
1127 was then added to the medium and cells were centrifuged 1 h later. The statistical

analysis was performed by using a t-test for all genes, with an exception for *tcdB*+acetate (Mann-Whitney test). C) Transcript levels of the *tcdA*, *tcdB* and *tcdR* genes of strain 630 $\Delta$ *erm* (white boxes) and 630 $\Delta$ *erm*::*CD2602* (black boxes) after exposure to pyruvate for 1 h, as described in panel A. qRT-PCR results are presented as the ratio between the amount of mRNA (arbitrary units) of each gene normalized by the DNA *polIII* gene from bacterial cells grown in PY supplemented with one of the compounds (pyruvate, Na<sub>2</sub>S, formate or acetate) compared to the amount of mRNA in the untreated cells. Data are the averages of at least three independent experiments (error bars are the standard deviations from the mean values). The statistical analysis was performed by using a t-test for all genes, with an exception for *tcdR*+pyruvate (Mann-Whitney test).

1138  
1139  
1140

**Table 1.** Strains and plasmids used in this study.

strains	background	knockout or overexpressed gene	plasmid	origin
630 $\Delta$ <i>erm</i>				87
M7404	BI/NAP1/027			2
M7404 ( <i>tcdC</i> <sup>+</sup> )	BI/NAP1/027		pDLL17 ( <i>tcdC</i> <sup>+</sup> )	2
VPI10463				Virginia Polytechnic Institute
CDIP001	630 $\Delta$ <i>erm</i>	<i>CD1287 (fur)::erm</i>		This study
CDIP106	630 $\Delta$ <i>erm</i>	<i>CD0278::erm</i>		This study
CDIP107	630 $\Delta$ <i>erm</i>	<i>CD2023::erm</i>		This study
CDIP110	630 $\Delta$ <i>erm</i>	<i>CD2065::erm</i>		This study
CDIP217	630 $\Delta$ <i>erm</i>	<i>CD3176 (sigL)::erm</i>		This study
CDIP342	630 $\Delta$ <i>erm</i>	<i>CD3176 (sigL)::erm</i>	pDIA6309	This study
CDIP540	630 $\Delta$ <i>erm</i>	<i>CD1594 (cysK)::erm</i>		This study
CDIP656	630 $\Delta$ <i>erm</i>		pDIA6456	This study
CDIP657	630 $\Delta$ <i>erm</i>	<i>CD2602::erm</i>		This study
JIR8094				88
CDIP100	JIR8094	<i>CD1064 (ccpA)::erm</i>		13
LB-CD15	JIR8094	<i>CD1275 (codY)::erm</i>	pBL92	Bouillaut et al., in prep
plasmids	vector	cloned gene	resistance	origin
pDIA5906	pMTL007	Intron <i>CD1287 (fur)</i>	<i>Cm, Tm</i>	This study
pDIA6309	pMTL84121	<i>CD3176 (sigL)</i>	<i>Cm, Tm</i>	This study
pDIA6450	pMTL007	Intron <i>CD0278</i>	<i>Cm, Tm</i>	This study
pDIA6451	pMTL007	Intron <i>CD2065</i>	<i>Cm, Tm</i>	This study
pDIA6452	pMTL007	Intron <i>CD2023</i>	<i>Cm, Tm</i>	This study

pDIA6453	pMTL007	Intron <i>CD3176</i>	<i>Cm, Tm</i>	This study
pDIA6454	pMTL007	Intron <i>CD2602</i>	<i>Cm, Tm</i>	This study
pDIA6455	pMTL007	Intron <i>CD1594 (cysK)</i>	<i>Cm, Tm</i>	This study
pDIA6456	pRPF185	AS <i>CD3029 (malY)</i>	<i>Cm, Tm</i>	This study

*Cm* : chloramphenicol; *Tm* : thiamphenicol; *Erm* : Erythromycin; AS : Antisens

**Table 2.** Growth of *C. difficile* strain 630 $\Delta$ *erm* in minimal medium containing different sulfur sources.

Sulfur source	Growth	
	16 h	48 h
Sulfate (4 mM)	-	-
Sulfite (4 mM)	-	-
Sulfide (4 mM)	+	+
Thiosulfate (4 mM)	-	+
Cysteine (4 mM)	+	+
Cystine (2 mM)	-	+
Glutathione (2 mM)	+	+
Cystathionine (2 mM)	-	+
Homocysteine (2 mM)	+	+
Methionine (1.5 mM)	-	-

+ indicates a growth and – an absence of growth

**Table 3.** List of the Fur-regulon genes that are differentially expressed in PY and PYC with a putative Fur box in their promoter region.

Gene	function	Ratio PYC/PY	Fur box
<i>CD1287 fur</i>	Ferric uptake regulation protein	3.3	- 38
<i>CD1477 feoA</i>	Ferrous iron transport protein A	64.1	
<i>CD1478 feoA1</i>	Ferrous iron transport protein A1	107.0	
<i>CD1479 feoB1</i>	Ferrous iron transport protein B1	127.1	- 60
<i>CD1480</i>	putative exported protein	162.6	
<i>CD1745A feoA</i>	Ferrous iron transport protein A	16.7	- 30
<i>CD3273 feoA3</i>	Ferrous iron transport protein A	13.4	- 30
<i>FCD3274 feoB3</i>	Ferrous iron transport protein B	12.1	
<i>CD2878 fhuD</i>	ABC transporter, ferrichrome substrate-binding protein;	N/A	- 47
<i>CD2875 fhuC</i>	Ferrichrome ABC transporter	3.0	
<i>CD1594 cysK</i>	O-acetyl-serine sulfhydrylase	43.0	- 162
<i>CD1595 cysE</i>	Serine acetyltransferase	44.0	
<i>CD1999 fldX</i>	Flavodoxin	28.5	- 158
<i>CD1777</i>	Putative arsenate reductase	3.3	- 80
<i>CD1485</i>	Conserved hypothetical protein	6.9	- 34
<i>CD2499</i>	Conserved hypothetical protein	15.4	- 34
<i>CD2881</i>	Conserved hypothetical protein	2.6	- 58

CD2992	Conserved hypothetical protein,	2.5	- 36
CD2991	ABC transporter, sulfonate-permease	3.5	
CD2989	ABC transporter, sulfonate-extracellular solute-binding protein	4.8	

1151

1152 The position of the Fur box is indicated according to the translational start site of the  
 1153 corresponding gene. N/A means “not detected in transcriptome”.

1154

1155

1156 **Table 4.** Effect of cysteine addition on the intracellular concentration of amino acids in strain  
 1157 630Δ*erm*.

1158

Amino-acids	PY (μmol/L)	PYC (μmol/L)	Ratio PYC/PY
<b>Up in the presence of cysteine</b>			
Leucine	ND	16.25 +/- 1.6	+
Tyrosine	ND	20 +/- 1.2	+
Alanine	13.5 +/- 0.7	748 +/- 40	55
Valine	5.3 +/- 0.5	56.8 +/- 1.3	10
Phenylalanine	2.6 +/- 0.5	25.75 +/- 5	10
Glutamic acid	19.3 +/- 2	121.9 +/- 9.5	6.5
Aminobutyric acid	8.5 +/- 0.5	46.35 +/- 0.8	5.5
Threonine	1.1 +/- 0.1	2.4 +/- 0.4	2.2
Serine	4 +/- 0	9.85 +/- 0.15	2.5
Asparagine	29.7 +/- 2.6	59.7 +/- 1.6	2
Methionine	4.85 +/- 0.35	11.65 +/- 1.65	2.5
<b>Down in the presence of cysteine</b>			
Cystathionine	1.2 +/- 0.2	ND	-
Glutamine	11.8 +/- 0.4	6 +/- 0.1	0.5
Hydroxyproline	23.3 +/- 1.5	13.9 +/- 0.5	0.6

1159 ND means not detectable

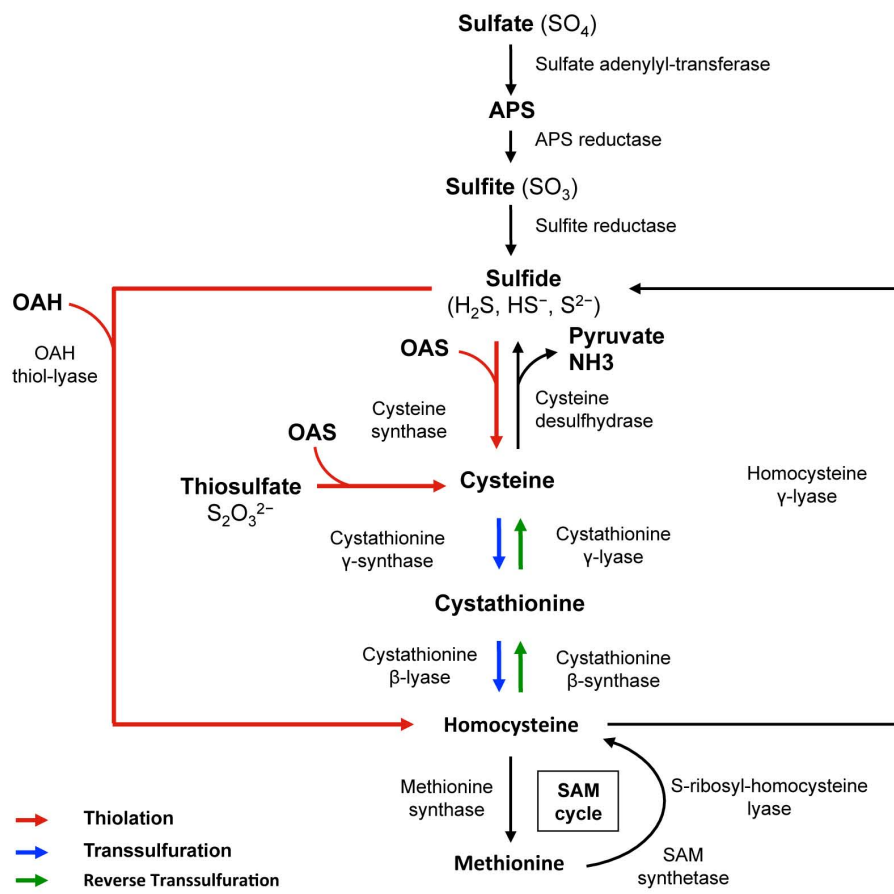


Fig. 1

